MÀSTER UNIVERSITARI EN OPTOMETRIA I CIÈNCIES DE LA VISIÓ

TRABAJO FINAL DE MÁSTER

ASYMMETRY OF RETINAL PHYSIOLOGICAL MEASUREMENTS IN YOUNG ADULTS MEASURED WITH OPTICAL COHERENCE TOMOGRAPHY

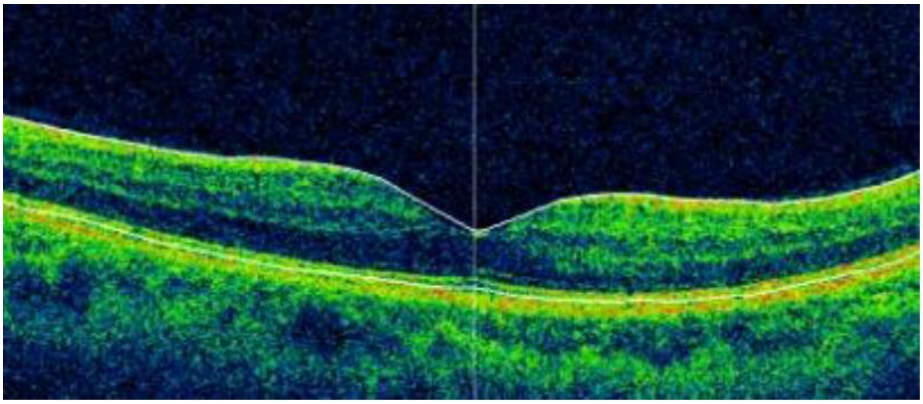

Zeyad A. Alzaben

DIRECTOR: Genís Cardona Torradeflot
DEPARTAMENTO: Òptica i Optometria

Junio, 2014

MÀSTER UNIVERSITARI EN OPTOMETRIA I CIÈNCIES DE LA VISIÓ

El Sr. Genís Cardona Torradeflot, como director del trabajo

CERTIFICA

Que el Sr. Zeyad A. Alzaben ha realizado bajo su supervisión el trabajo "Asymmetry of Retinal Physiological Measurements in Young Adults Measured with Optical Coherence Tomography", que se recoge en esta memoria para optar al título de máster en optometría y ciencias de la visión.

Y para que conste, firmo este certificado.

Sr Genís Cardona Torradeflot
Director del trabajo

Terrassa, 13 de Junio de 2014

MÁSTER UNIVERSITARIO EN OPTOMETRIA Y CIENCIAS DE LA VISIÓN

ASYMMETRY OF RETINAL PHYSIOLOGICAL MEASUREMENTS IN YOUNG ADULTS MEASURED WITH OPTICAL COHERENCE TOMOGRAPHY

SUMMARY

Introduction: Optical coherence tomography (OCT) is a useful technique to assess the retina. In this study, we explored the physiological inter-ocular asymmetry of several retinal parameters in a sample of young Caucasian adults.

Methods: A transversal study was designed in which the macular exploration protocol of the 3D-OCT-2000 was employed to evaluate several retinal parameters in a sample of 37 young adults aged between 12 and 23 years (spherical equivalent from -3.00 to +4.00 D). Normal inter-ocular asymmetry values were determined and compared with previous published tolerance values.

Results: Statically significant differences were found between males and females in mean thickness of the retinal nerve fibre layer (RNFL) in the right eye. In addition, Inter-ocular statistically significant differences were uncovered in mean and superior RNFL thickness, as well as in central macular thickness (all $p<0.05$). Mean RNFL thickness for the left eye was higher than for the right eye by 1.70 µm.

Conclusions: The exploration of the normal asymmetries of the retina may be an effective approach for an early detection of pathologies of the retina such as glaucoma. Differences in instrumentation and sample characteristics do not allow for a direct comparison between the present findings and previous research.

MÁSTER UNIVERSITARIO EN OPTOMETRIA Y CIENCIAS DE LA VISIÓN

ASIMETRIA FISIOLÒGICA DELS PARÀMETRES DE LA RETINA EN UN GRUP D'ADULTS JOVES, MESURADA MITJANÇANT TOMOGRAFIA DE COHEREÈNCIA ÒPTICA (OCT)

RESUM

Introducció: La tomografia de coherència òptica (OCT) és una tècnica útil per explorar la retina. En aquest estudi s'avaluà l'asimetria fisiològica inter-ocular de diversos paràmetres de la retina en una mostra de adults joves caucàsics.

Mètodes: Es dissenyà un estudi transversal emprant el protocol d'exploració macular del 3D-OCT-2000 per avaluar diversos paràmetres de la retina en una mostra de 37 subjectes d'edats compreses entre 12 i 23 anys (equivalent esfèric: -3,00D a +4,00D). Es calcularen els valors normals d'asimetria inter-ocular i es compararen amb els límits de tolerància prèviament publicats.

Resultats: Es trobaren diferències estadísticament significatives entre homes i dones en la mitjana del gruix de la capa de fibres nervioses de la retina (RNFL) de l'ull dret. A més, s'obtingueren diferències estadísticament significatives entre ambdós ulls en la mitjana del gruix de la RNFL, així com en el gruix del quadrant superior i del centre macular ($p<0,05$). La mitjana de gruix de la RNFL de l'ull esquerra fou major en 1,70µm.

Conclusions: L'exploració de l'asimetria normal de la retina pot ser efectiva per la detecció precoç de patologies de la retina com el glaucoma. Les diferències en instrumentació i característiques de la mostra dificulten comparacions amb estudis previs.

MÁSTER UNIVERSITARIO EN OPTOMETRIA Y CIENCIAS DE LA VISIÓN

ASIMETRÍA FISIOLÓGICA DE LOS PARÁMETROS DE LA RETINA EN UN GRUPO DE ADULTOS JÓVENES, MEDIDA MEDIANTE TOMOGRAFÍA DE COHERENCIA ÓPTICA (OCT)

RESUMEN

Introducción: La tomografía de coherencia óptica (OCT) es una técnica útil para explorar la retina. En este estudio se evaluó la asimetría fisiológica inter-ocular de varios parámetros de la retina en una muestra de adultos jóvenes caucásicos.

Métodos: Se diseñó un estudio transversal usando el protocolo de exploración macular del 3D-OCT-2000 para evaluar varios parámetros de la retina en una muestra de 37 sujetos de edades comprendidas entre 12 y 23 años (equivalente esférico: -3,00D a +4,00D). Se calcularon los valores normales de asimetría inter-ocular y se compararon con los límites de tolerancia publicados.

Resultados: Se hallaron diferencias estadísticamente significativas entre hombres y mujeres en el promedio del grosor de la capa de fibras nerviosas de la retina (RNFL) en ojo derecho. Además, se obtuvieron diferencias estadísticas entre ambos ojos en el promedio del espesor de la RNFL, así como en el grosor del cuadrante superior y del centro macular ($p<0,05$). El promedio de grosor de la RNFL en ojo izquierdo fue mayor en 1,70µm.

Conclusiones: La exploración de la asimetría normal de la retina puede ser efectiva en la detección prematura de patologías de la retina como el glaucoma. Diferencias en instrumentación y muestra dificultan comparaciones con estudios previos.

Acknowledgements

First I want to thank the director of this work, Genís Cardona, and my dear uncle, Ahmad Zaben Omran, for giving me the opportunity to do this work which has helped me to have more global overview of the visual therapy.

Thanks Dana N. Koff, Izdihar Alsalman, Mira F Haddad, Mayy Bakkar, Suha Abu Saif, and Areej Otum that have qualified me passing from Bachelor degree to the Master degree. As well to my loyal friend Ayman R. Bsharat.

Thanks to the company Optipunt Zaben (Figueres) for the contribution of collecting the data for this study.

And thanks to my partners of the Master, by turning 1 year of stress and exhaustion, into peace and hugs.

Thanks to my fabulous team in Spain who have worked hard to bring my skills into this level: Aurora Torrents, Eulalia Sánchez, Montserrat Morató, Vanesa Budi, Mónica Hernández, Ferran Casals, Dr. Xavier Corretger, Dr. Sanchez Dalmau, and the other partners in the Hospital Clínic de Barcelona.

Extra special thanks to my former teacher, Fatiha Assaf

Finally to my close family: my parents, my sisters, my uncles and my grandparents.

To all,

Thanks

Ze Yad

Contents

1. Introduction

The health of the fundus of the eye is critical to ensure good vision. This area contains the retina, which includes the optic nerve head, the macula and the fovea. The ophthalmological evaluation of the fundus is very relevant due the valuable information regarding ocular or systemic diseases that may be obtained by this exploration.

New instrumentation based on the interferometry principle has been developed. Such an instrument is the optical coherence tomographer (OCT), a non-invasive technique using low coherence interferometry, which allows real time *in vivo* acquisition of retinal images akin to ocular biopsy. This device is used to evaluate the posterior segment of the eye to assess the optic nerve head quantitatively, the retinal nerve fiber layer, and the macular thickness. Also, it is widely used for the diagnosis and follow-up of patients who suffer from retinal alterations such as cystoids macular oedema, glaucoma and age-related macular degenerations.

OCT offers a longitudinal resolution of 5 microns, which is considered as the most highly resolved images of the *in vivo* retina, in comparison with other imaging techniques. There are various types of OCT commercially available with differences in the time needed to acquire the image, depth of focus, and resolution. The OCT integrated by Topcon analyzes the retina using 3D imaging, reducing the noise to provide extremely detailed results, throughout a non-mydriatic digital camera with less than 1 millisecond of flash at the moment of capturing the image.

In this study we will describe the anatomical aspects of the ocular fundus, the normal and abnormal signs of several ophthalmological conditions, the most commonly used instruments to assess the fundus, and the direct retinal imagine technique offered by the OCT, highlighting on the key differences between normal and abnormal ocular conditions.

Any physiological asymmetry of retinal parameters between the right eye and the left eye of the same person may be considered a key to rule out certain unilateral or asymmetrical diseases such as glaucoma or tumours of the optic nerve. In the present study we have employed the OCT (3D-2000 Topcon) on a sample of young adults to assess the normal physiological asymmetry of some retinal parameters for European-Caucasian subjects.

2. Theoretical Framework

2.1. Retinal Anatomy of Human Eye and Mechanisms of Some Retinal Disease

The retina, which is considered the gate of 80% of the sensory information reaching our brain, is located in the posterior pole of the eye and can be classified in order to its schematic location as central retina and peripheral retina. The retina consists of 10 distinct layers (**Figure 2.1)**.

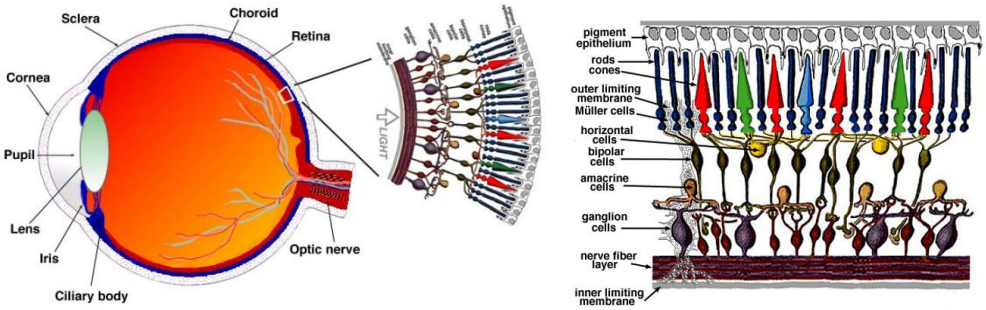

Figure 2.1. Anatomical structure of the human retina (From: http://webvision.med.utah.edu/)

The retina contains two types of photoreceptors, rods and cones, which transmit the neural impulses via the optic nerve to the visual cortex in the brain for further processing. The central part of the retina, called the macula, is responsible for the sharpest vision and colour discrimination. In adults it is 1.5 mm in diameter and located 3 mm temporally to the optic disc, and it is also denoted by the name of *macula lutea* due to the presence of xanthophyll, a yellow carotenoid pigment. The fovea, which is located at the central part of the macula within a 0.35 mm wide depression, is responsible for the greatest visual acuity.

Clinical examination is required to evaluate the reflex of the fovea as any loss of this reflex may indicate early macular disease. The foveola, located at the centre of the fovea, has the highest density of cone photoreceptors (199,000 / mm^2), which are characterized by their elongated and narrow shape. The development process of the

fovea represents the inward migration of the cone photoreceptors and the outward displacement of the cells from the inner nuclear and ganglion cell layers. In most fundus images the macula is represented by a darker region (**Figure 2.2**). (1)

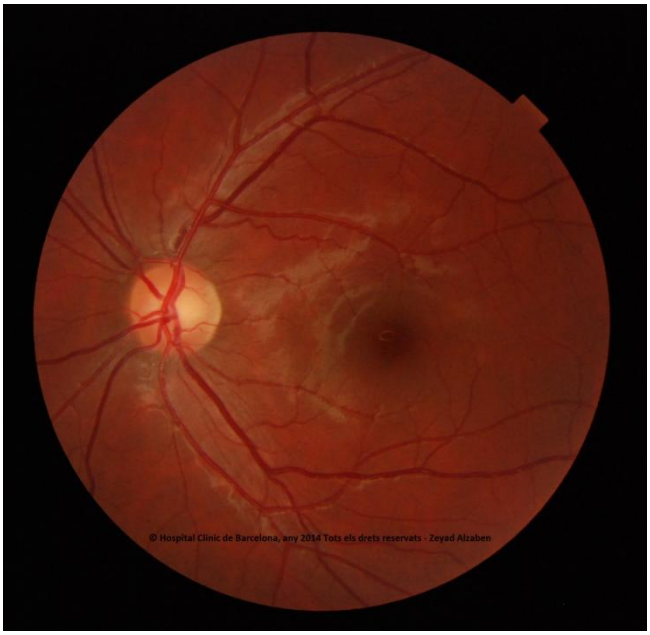

Figure 2.2. Observation of the normal ocular fundus. Please note the optic disc (yellow/white, origin of blood vessels) and the macula (avascular darker area)

The fovea is considered a rod-free zone and the foveola contains only cone photoreceptors and Müller cells. Also, the central 500 microns of the fovea are excluded from retinal capillaries (*foveal avascular zone or FAZ*), with nourishment being provided by the blood supply from the choriocapillaries. (2)

The peripheral retina represents the region of the retina, which extends from the borders of the macula and the optic disc towards the ora serrata, that plays an important role in the spatial orientation process of visual perception in addition to the stabilization of vision during movement and under scotopic conditions. There are several ocular pathologies characterized by morphological changes appearing in the periphery first, such as retinitis pigmentosa, diabetic retinopathy, and some types of uveitis. (3)

The optic disc represents the place from which the retinal vessels and nerve axons enter and leave the eye. It is also the brightest area in the retinal image, nearly oval in shape. The optic disc should be evaluated to assess the morphology of blood vessels in that area, as well as a landmark to measure distances for different anatomical parts of the retina. Indeed, some authors use the spatial relationship between the optic disc diameter and the region of the macula to locate the fovea. The shape, colour, and depth of the optic disc are considered hallmarks for the detection of various ocular diseases such as glaucoma and diabetic retinopathies. The size of the optic disc in the fundus image usually occupies about one seventh of the image, although this size may vary from one person to another. The neuroretinal rim is the boundary between the optic nerve head and the retina. (6)

The retina is about 250 micrometers thick, with 10 layers from the innermost to outermost retina (**Figure 2.1** and **Figure 2.3**):

1- Internal Limiting Membrane (ILM): it represents the interface between the retina and the vitreous. It contains astrocytes and the end of Müller cells.
2- Retinal Nerve Fibres Layer (RNFL): it is a myelinated layer consisting on the axons of retinal ganglion cells.
3- Ganglion Cells Layer (GCL): it receives the visual information from rods and cones via intermediate nerve cells (bipolar cells and amacrine cells). The ganglion cells are responsible for transmitting the visual information to the brain.
4- Inner Plexiform Layer (IPL): it is the layer where bipolar, amacrine, and ganglion cells are interacting in the process of visual perception.
5- Inner Nuclear Layer (INL): this layer is characterized by closely packed bipolar, horizontal and amacrine cells.
6- Outer Plexiform Layer (OPL): it contains a dense network of neural synapses between the horizontal cells from INL and the inner segments of the photoreceptors from the outer nuclear layer.
7- Outer Nuclear Layer (ONL): it contains several oval nuclear bodies, rod and cone granules.

8- External Limiting Membrane (ELM): Its role is to act as a skeleton to maintain the alignment of the photoreceptor cells.
9- Photoreceptors layer: it is the layer of retina where cones and rods are located.
10- Retinal Pigmented Epithelium (RPE): Arising from the neuroectoderm, it supports the function of rods and cones.

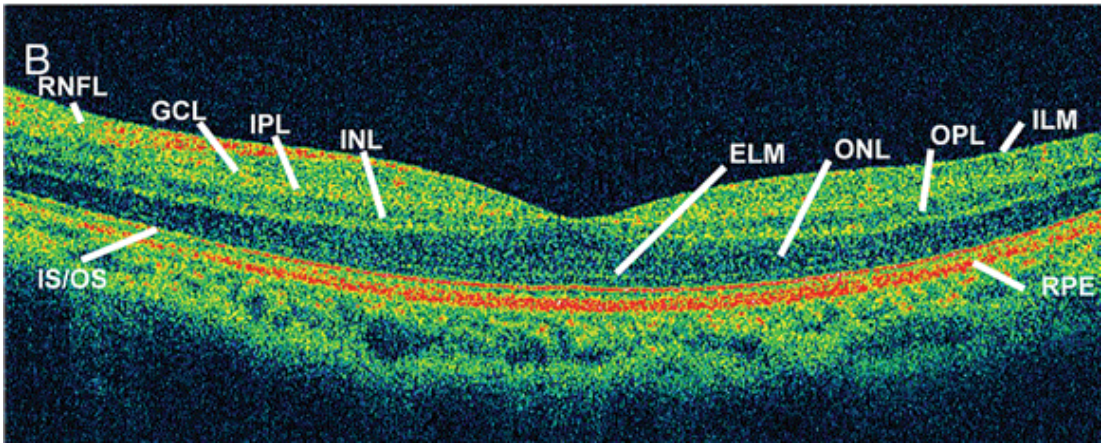

Figure 2.3. Image obtained with coherence tomography showing all retinal layers

2.2. Common retinal pathologies

Some of the most common pathologies that may affect the retina and surrounding structures are described below. Many of these pathologies will result in a modification in one or various retinal structures that should be easily detected with the adequate equipment.

Glaucoma is a neurological degenerative chronic disease, largely asymptomatic, that represents a group of ocular conditions may damage the optic nerve due to an increase in intraocular pressure (IOP) originating in a blockage of the flow of aqueous humour. It may be classified into four main types: (7)

a. Chronic open angle glaucoma (the most common type) also called primary open angle glaucoma: it is usually the result of raised IOP within the eye, and may lead to visual loss or blindness if left untreated. It develops slowly with a gradual loss of vision.

b. Acute close angle glaucoma (painful): it is a more uncommon type of condition characterized by a narrowing of the angle between the iris and the sclera and a sudden increased in IOP within the eye.
c. Congenital glaucoma, where the glaucoma is presented from birth.
d. Secondary glaucoma: it may be caused by complications of some eye injuries, be related to some drugs like corticosteroids or to ocular diseases like uveitis.

The optic nerve head is very sensitive to any changes in the pressure of the eye associated with glaucoma (**Figure 2.4**), and damage may be irreversible. Therefore, treatment aims at reducing or preventing further effects of the disease. Risk factors for glaucoma may be related to race, sex, age, high myopia, and IOP. (8)

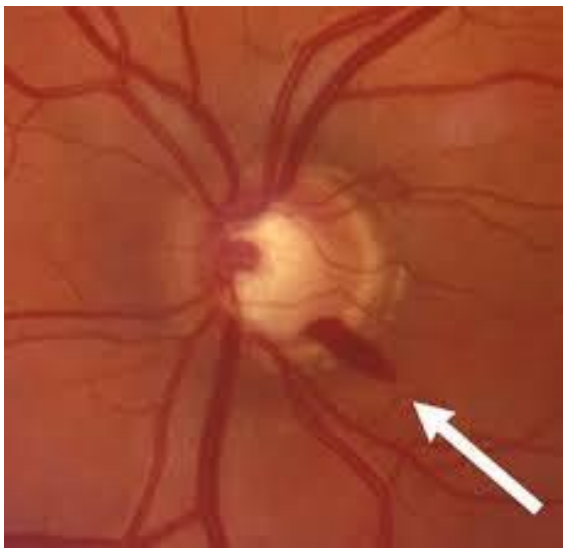

Figure 2.4. Optic nerve haemorrhage associated with glaucoma (From: http://web.mst.edu/)

Age-related macular degeneration (ARMD or AMD) is an untreatable progressive condition of the eye that leads to blindness with a prevalence that increases with age. It is considered more common in females, and in the less-pigmented races. It may be classified into dry (chronic) or wet AMD, with different prognosis. It is asymptomatic during the early stages, which may present an accumulation of drusen over the retina **Figure 2.5**), while the late stage of the dry type, often denoted by the term of geographic atrophy (GA), is characterized by retinal pigment epithelial cells

degeneration. The wet type of AMD is associated with the presence of choroidal neovascularization (CNV), leading to the accumulation of fluid leaked from these new fragile vessels below or within the retina, (9). Major risk factors of AMD include smoking, obesity, race, sex, and family history.

Figure 2.5. Age-related Macular Degeneration with clearly visible drusen (From: http://www.nysoa.org/)

Macular Hole is an untreatable condition that leads to central vision loss, due to tangential traction of the vitreous. It is clinically characterized by a localized separation of the posterior vitreous with the adherence impact between the fovea-vitreous interface in eyes with stage 1 and stage 2 as classified by Gass (10). It displays a pre-foveal opacity as a result of centrifugal photoreceptor displacement (**Figure 2.6**). The stages of this condition can be summarized as follows:

1. Impending macular hole
2. Early full-thickness hole with or without an attached operculum
3. Full-thickness hole
4. Full-thickness hole with complete separation of the posterior hyaloids through the macula and optic disc

High myopia is a risk factor of macular hole due to increased axial length of the eye.

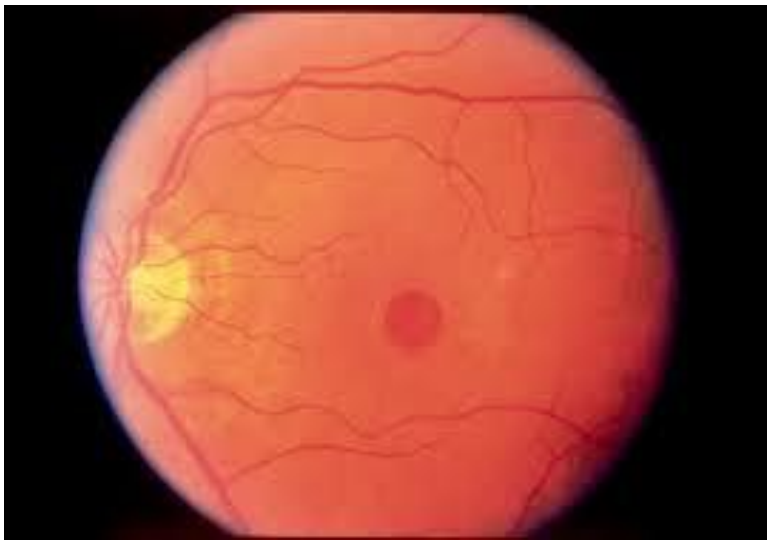

Figure 2.6. Macular Hole (From: http://www.avclinic.com/)

Diabetic retinopathy is a bilateral condition in which there is an abnormal growth of fragile blood vessels on the surface of the retina (**Figure 2.7**). It may be classified into nonproliferative (NPDR) and proliferative (PDR) diabetic retinopathy. Whereas NPDR, also known as background retinopathy, is the early stage of diabetic retinopathy characterized by the appearance of tiny blood vessels within the retina associated with blood leakage resulting in swelling of the retina, PDR occurs when abnormal blood vessels starts to grow on the retinal surface of on the optic nerve, which do not supply the retina with normal flow of blood. (11)

Macular oedema is a common ocular disease that leads to loss of vision due to the abnormal accumulation of fluid within the retina, resulting in a concomitant increase in the retinal thickness after the breakdown of the blood-retinal barrier (**Figure 2.8**). This condition may be found in patients with diabetic retinopathy, retinal vein occlusion, and uveitis. (12)

Figure 2.7. Diabetic Retinopathy (From: http://www.neec.com/)

Figure 2.8. Macular Oedema (From: www.willseye.org)

Epiretinal membrane is an ocular condition in which there is a thin layer of scar tissue on the surface of the macula, leading to blurred vision (**Figure 2.9**). The presence of an epiretinal membrane may be related to normal aging of the eye, or to other conditions such as diabetes, thrombosis, after retinal surgery, or inflammation. (13)

Figure 2.9. Epiretinal Membrane (From: http://webeye.ophth.uiowa.edu/)

Finally, ***Central serous chorioretinopathy*** is a common disease characterized mainly by the accumulation of subretinal fluid in the posterior pole of the eye, resulting in a circumscribed area of serous retinal detachment. It is more common in middle-aged men. (14)

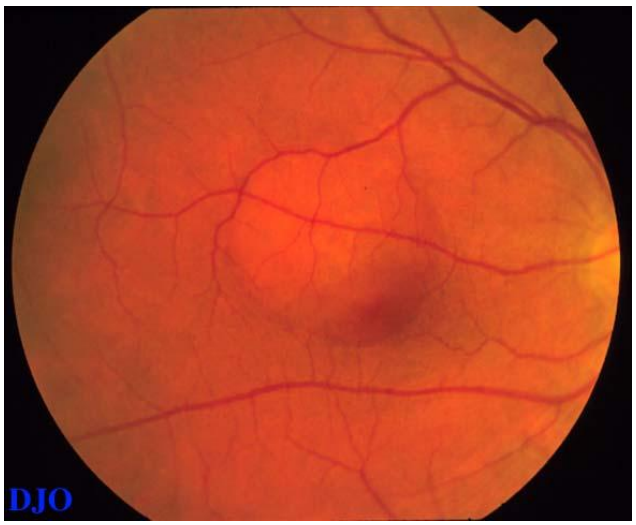

Figure 2.10. Central Serous Chorioretinopathy (From: http://www.djo.harvard.edu/)

2.3. Special Testing Techniques and Instruments for retinal exploration

These instruments allow the examiner to detect ocular pathologies, and reveal characteristics of a variety of underlying systemic pathologies of the retina.

2.3.1. Direct Ophthalmoscope

It was first proposed in 1827 by Jan Evangelista Purkinje, invented in 1847 by Charles Babbage, and first used in a clinical setting in 1851 by Hermann von Helmholtz. This device allows for the observation of the ocular fundus and for the assessment of the optic disc. The direct ophthalmoscopy is considered a familiar, easy to use, commonly available instrument that permits the identification of many ocular pathologies such as papilloedema, glaucomatous optic neuropathy, diabetic neuropathy, hypertensive retinopathy, cataract, vitreous haemorrhage, and age-related macular degeneration.

This instrument contains a set of lenses that focus a tungsten halogen light of 2.5v in power on to a mirror or prism to further reflect it as a diverging beam to illuminate the structure of the eye (**Figure 2.11**), producing an upright image of 15X magnification (in an emmetrope) and a field of view of 2 disc diameters (about 5°). The device also contains a series of corrective lenses to compensate the refractive errors of either the patient or the examiner. The examination is carried out in a darkened room, without the need for pupil dilation. (15)

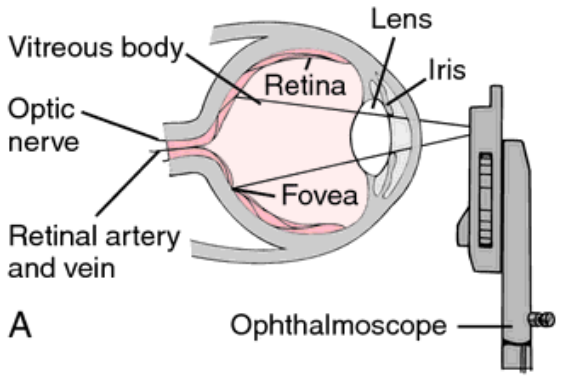

Figure 2.11. Direct ophthalmoscope (From: http://medical-dictionary.thefreedictionary.com/)

The direct ophthalmoscope may be used to differentiate between the true papilloedema and pseudopapilloedema, which the later is characterized by apparent swelling of the optic disc secondary to underlying benign condition instead of being secondary to raised IOP, since the clinician may observe spontaneous venous pulsation at the optic disc that is absent in true papilloedema, which suggests closure of the central retinal vein (**Figure 2.12**). This condition is not easily seen with fundus examination using slit-lamp biomicroscopy. (16)

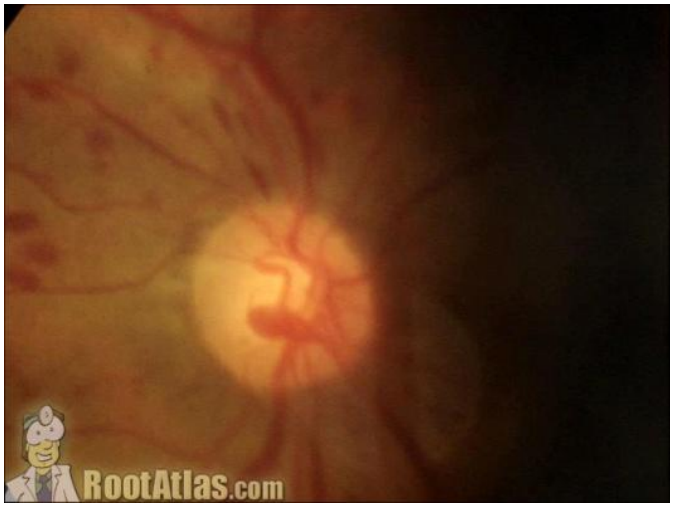

Figure 2.12. Spontaneous venous pulsation (From: http://www.rootatlas.com/)

The disadvantages of the direct ophthalmoscope are:

1. It provides two dimensional images (2-D), thus it is not valid in comparing the cup-to-disc ratio or macular oedema since it does not present a stereo view.
2. It has a fixed low magnification.
3. There is a limited illumination level.
4. It requires a very close working distance.
5. Significant posterior pole lesions of the eye can be missed due to the difficulties in scanning the retinal surface, in addition to the small field of view.

2.3.2. Indirect Monocular Ophthalmoscope (MIO)

This device is very useful during fundus examination in young patients with strabismus or amblyopia in order to figure out their organic cause. It uses a direct ophthalmoscope in conjunction with a +20.00 dioptres lens placed 3 to 5 cm in front of the eye of the patient (**Figure 2.13**). This allows for a larger field of view, and a moderately magnified view of the fundus, as well as avoiding the close distance between the patient and the examiner required for direct ophthalmoscopy. Therefore, it minimizes the difficulties encountered with non-cooperative patients like children. (17)

Figure 2.13. Hand-held indirect monocular ophthalmoscope (From: http://www.heine.com)

Also, indirect ophthalmoscopy is commonly used in those countries in which optometrists are not legally allowed to use mydriatic agents, or with patients who do not tolerable to bright light of the binocular technique (*see below*), as well as when the examiner has monocular vision. It provides an upright image with a field of view of 25° of the fundus with 15X magnification, or 17.5° field of view with 22X magnification. This type of ophthalmoscope still presents a 2-D image, though. (18)

2.3.3. Headband Binocular Indirect Ophthalmoscope (BIO)

The BIO offers a fast technique for the assessment of the entire fundus (equatorial, midperipheral and peripheral areas). It uses a +20.00 diopters lens and requires pupil dilation for better observation (**Figure 2.13**). This technique is optimal in the diagnosis of retinal holes or tears, retinal detachment, intraretinal haemorrhages, exudates, vitreoretinal traction, naevi and tumours. (19)

The BIO allows for the examination of the posterior pole with a stereoscopic view of approximately 8 disc diameters (35°), as well as providing an improved view through ocular media opacities. (20)

Figure 2.13. Headband Binocular Indirect Ophthalmoscope used for ocular fundus exploration (From: http://www.indiamart.com/)

The advantages of this technique, however, are limited by the following factors:

1. It provides a real, inverted image of the fundus.
2. Pupil dilatation is usually required.
3. Supine position is required for the patient.
4. Patient may present photosensitivity.

2.3.4. Fluorescein Angiography (FA)

This procedure is a diagnostic method for ocular fundus examination that requires an intravenous injection of 2-5 cm^3 of sodium fluorescein dye and a specialized camera. It has an important role in diabetic retinopathy staging, and in the identification of leakage sources in the macular area, thus offering detailed information for laser treatment. The test relies on a dye tracing method to detect vascular changes around the macula with a blue 490 nanometres in wavelength light. There are two distinct sources of retinal blood supply:

1. Choriocapillaries supplying the outer retina.
2. Central retinal artery supplying the inner retina.

In diabetic retinopathy the foveal avascular zone (FAZ) presents with irregular margins and enlargement. In addition, diabetes results in reduced choroidal circulation that leads to hypoxia of the outer retina.

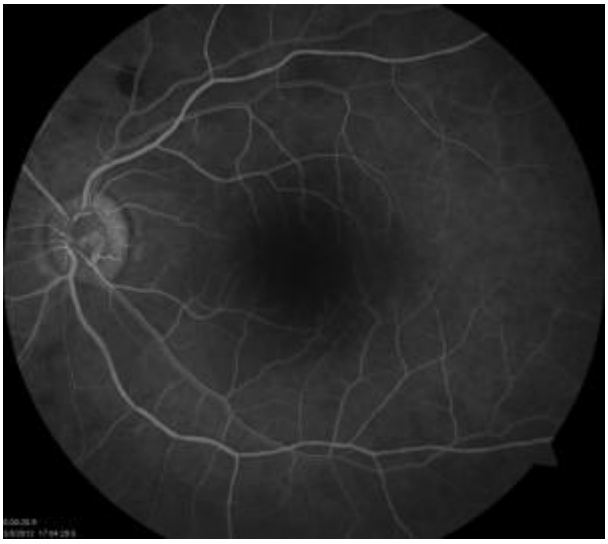

Figure 2.14. Fluorescein Angiography (From: http://www.retinaeyedoctor.com/)

Therefore, FAZ plays an important role in evaluating the capillary loss, reflects ischemic processes, and blood supply insufficiency to the inner retina. It must be noted that fluorescein reaches the retinal circulation 10 seconds after the intravenous injection.

Therefore, the examiner needs to capture images of the retina every second until 20 seconds after the injection, and delay images at 10 minutes and 15 minutes as well.

2.3.5. Indirect Fundus Biomicroscopy

This is a standard technique for the assessment of the posterior pole of the eye including the optic disc, macula, and the vasculature. The procedure, in which a high plus lens (+90.00 or +78.00 D) is used in conjunction with the slit-lamp, provides a stereoscopic view of the ocular fundus (inverted image) through dilated or non-dilated pupils, with a large field of view. The beam light should be about 2 mm wide and 7 mm high, while the lens is positioned 1 cm in front of the eye of the patient. (21)

This technique plays an important role in the assessment of the cup-to-disc ratio in glaucomatous eyes, and it may considered the best method for observing the fundus when ocular media opacities such as cataracts are present.

Figure 2.15. Indirect ophthalmoscope with slit-lamp biomicroscopy (From: Optonet)

2.3.6. Optical Coherence Tomography (OCT)

Optical coherence tomography is a very useful technique for the evaluation of glaucomatous eyes. Exploration involves examining a concentric circle which encompasses the optic disc, also taking into account the thickness of the retinal nerve fibres layer, although the variability in the size and appearance of the optic nerve head in normal eyes makes the detection of the first glaucomatous damage to the optic disc relatively difficult. The Identification of the structural damage of the glaucomatous optic nerve is important for the diagnosis, treatment, and follow-up of the clinical course of this condition. (7) (22)

The OCT is a non-invasive diagnostic and objective ocular imaging device giving cross-sectional high-resolution (maximum of 5 microns) and quantifiable images of both the anterior segment and the posterior pole. Thus, the OCT is similar to B-scan ultrasound, but the OCT measures light instead of acoustic waves.

The principles of this instrument are based on Michelson low coherence interferometry. A low coherent light from a superluminescent diode source (SLD) passes through a beam splitter and is separated into a reference beam and an explorer beam, which is then projected on the retina to be reflected back to the instrument. (23). The light backscattered by the various retinal tissues interferes with the light from the reference beam and information on the path of the backscattered light, and thus of the retinal layers, is obtained. The OCT principle has evolved from a time-domain to a spectral-domain, which has resulted in a notable improvement in image quality and diagnostic accuracy (compare **Figure 2.16** and **Figure 2.17**): (24)

1. Spectral-Domain (Fourier-Domain): This domain allows for the simultaneous exploration of layers at different depths, through 1024 A-scans in 0.04 seconds with a resolution of 5 microns.
2. Time-Domain: This domain explores various depths sequentially, through 512 A-scans in 1.28 seconds with a resolution of 10 microns.

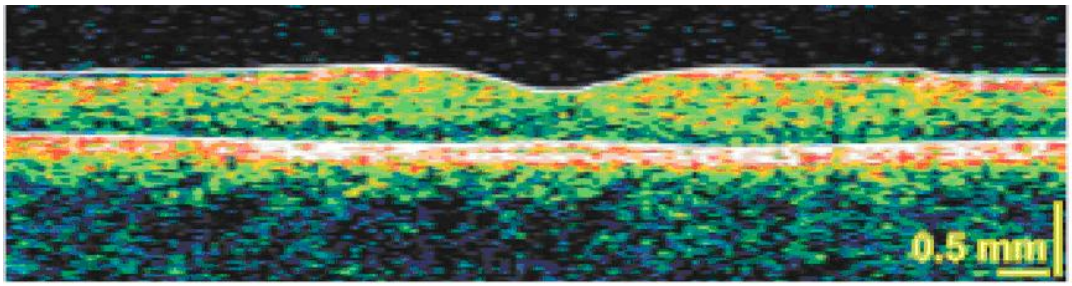

Figure 2.16. View of the normal macula using a Stratus OCT with a time-domain approach (From: http://www.gig.pitt.edu/)

It may be noticed that the detection based on time-domain is slower than eye movements, and vice versa for the spectral-domain detection type of OCT. In this study we are using spectral-domain 3D OCT-2000 (Topcon), which will be described in further detail in the Methods section. (25)

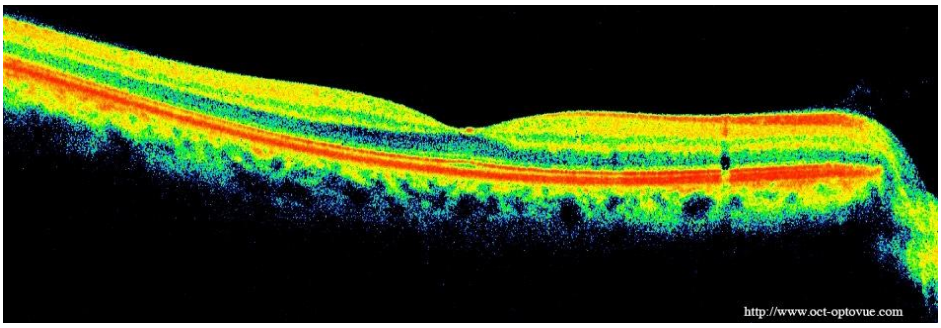

Figure 2.17. View of the normal macula using a spectral domain approach (From: http://www.oct-optovue.com/)

-Interpretation of OCT maps:

The OCT contains several algorithms to automatically calculate retinal thickness, and to analyze the optic nerve head (ONH) morphology, its size and the cup/disc ratio (C/D). The optic disc has a pinkish orange rim with a lighter colour at the centre, known as the neuroretinal rim or cup, with a C/D ratio within the range of 0.3-0.4 (*i.e.* one third of the height of the optic disc). (26) Other C/D ratios (see **Figure 2.18**) may be indicative of abnormality, although it may not always be the case (see, for example,

Figure 2.18. D, which, with a higher C/D ratio, may be normal if the patient is young or in has myopia). (27)

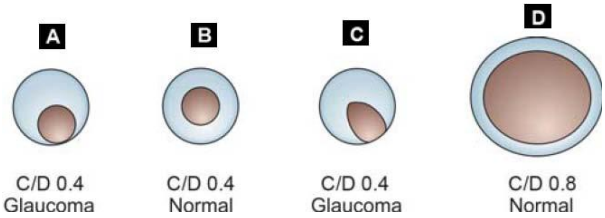

Figure 2.18. Cup / Disc ratio (From: http://www.jaypeejournals.com/)

The OCT also allows for the scan in three dimensions of the anterior segment in order to estimate the cornea-iris angle (**Figure 2.19**), as well as the posterior pole of the eye to explore through transversal images of the different layers of the retina, the macula, optic nerve head (ONH), the RPE layer, and the vitreoretinal interface. (27)

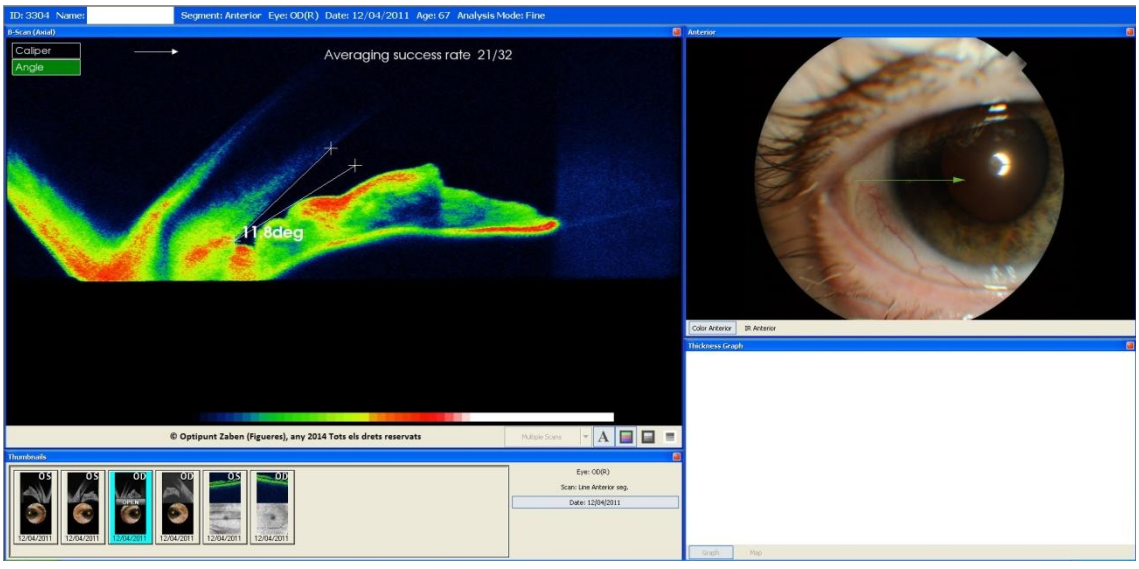

Figure 1.19. Corneal-Iris angle

Some examples of images obtained with the OCT are shown next (**Figure 2.20** and **Figure 2.21**). It may be observed that different layers of the retina offer different light

reflectivity, allowing for their identification. The OCT also provides with a detailed exploration of the optic nerve head (see **Figure 2.22**).

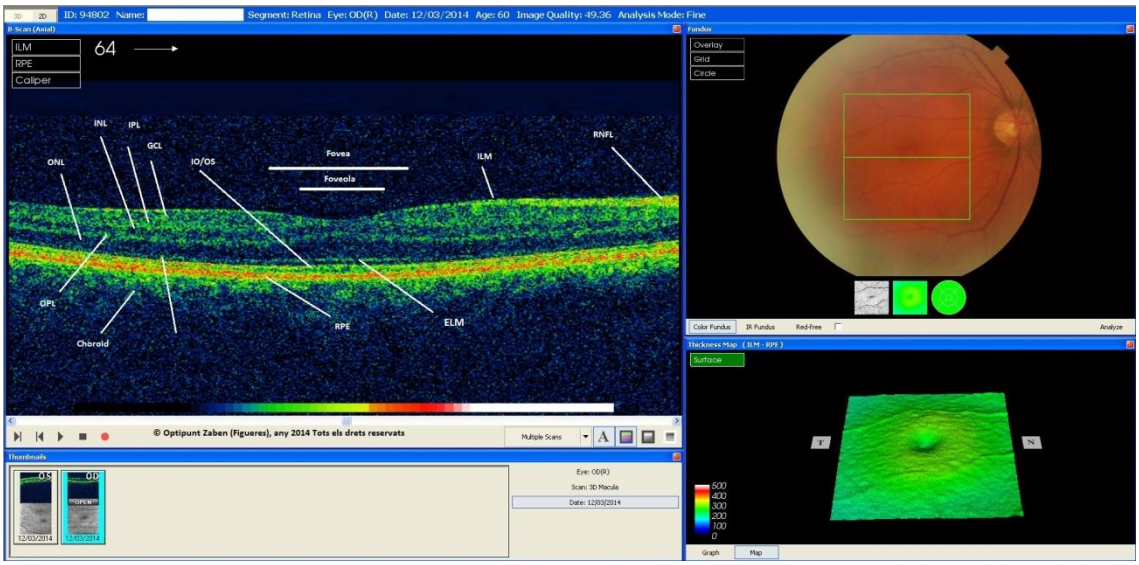

Figure 2.20. Normal OCT image of the macula

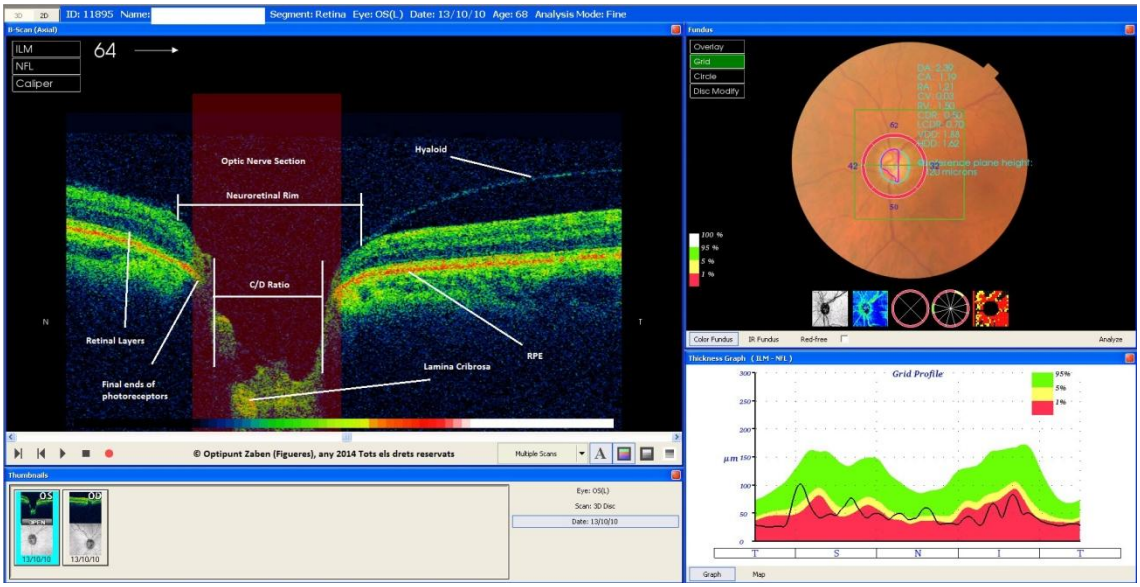

Figure 2.21. OCT image of a glaucomatous optic nerve

Colours are assigned depending on the reflectivity of the retinal tissues some, allowing for the detection of any abnormality in an OCT image. In addition, in case of low resolution colours are not affected, thus the appearance of the map is similar. The instrument also shows a scale from zero to ten of the resolution for the captured image, relying on the form of the contours of the posterior pole.

Retinal reflectivity in OCT maps may be interpreted as follows (28):

1. Retinal tissues with high reflectivity such as RPE/Choriocapillaries complex, the junction of the interior/exterior segments of photoreceptor, RNFL, and blood vessels are represented in red.
2. Retinal tissues with moderate reflectivity are represented in yellow-green colour: ELM, OPL, and IPL.
3. Retinal tissues with low reflectivity such ONL, INL, and GCL as are represented in blue.
4. Other tissues without reflectivity are represented in black colour: vitreous cavity.

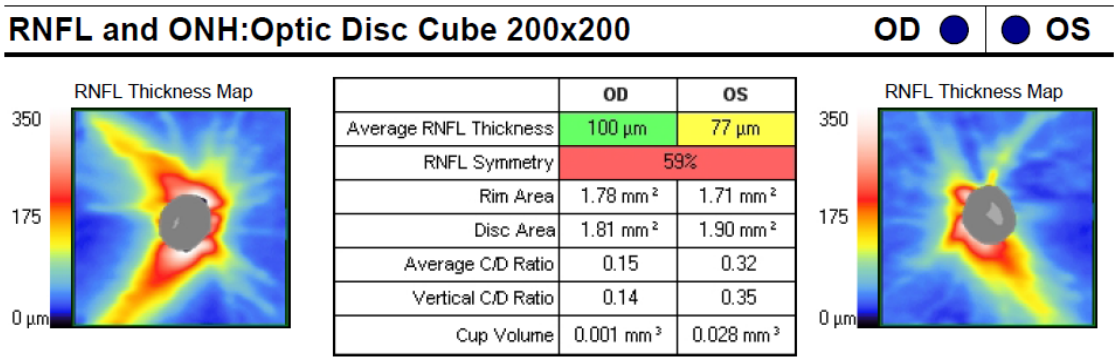

Figure 2.22. OCT exploration of the ONH

The OCT employs two main types of protocols in retinal assessment to explore for risk of glaucoma and to give a more general view of the retina and the various conditions (29).

-Clinical application for glaucoma

It is valuable to the examiner to have an objective measurement of the optic nerve structure (30). The OCT can evaluate RNFL thickness non-invasively and present it in four quadrants or mimicking the clock positions in relation to the optic nerve. Thus, the OCT is a great instrument to assess the early glaucomatous retina. The typical early glaucomatous finding is a superior-inferior thinning (**Figure 2.23**).

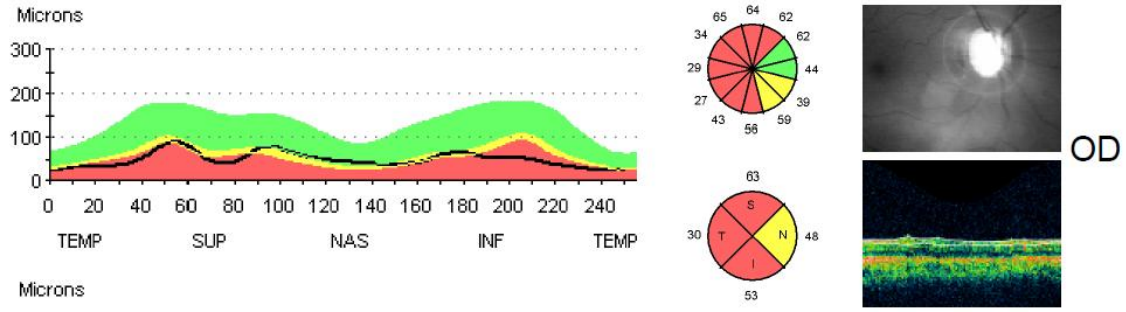

Figure 2.23. Severe decreased retinal thickness in glaucoma (right eye)

Optical coherence tomography offers a high reliability for the proper control of optic nerve changes, especially in atrophic conditions like glaucoma and Leber hereditary optic neuropathy. It is necessary to take into account the diagnostic importance of the OCT to discover the first stages of glaucoma in clinical practice. The evaluation of the RNFL, IOP, and the visual field should be able to provide adequate measurements for detecting glaucoma. Notice that in a normal macular image the nasal part of the RNFL has a higher reflectivity due to its position towards the optic nerve head.

-Clinical application for the diagnosis of macular and retinal diseases

OCT is considered a useful diagnostic tool in our clinic to evaluate macular pathologies such as macular oedema, macular holes, CSR, and ARMD (31). A retinal fundus image, as seen above, if complemented with an OCT scan, allow for a greatly improved diagnostic accuracy.

A ***macular hole*** in an OCT scan is characterized by the symmetrical borders of the hole, and the depth of the RPE layer (**Figure 2.24**)**.** A hyaloids detachment may be seen, and it is not uncommon to also observe the operculum, which is a detached part from the retina detected at the level of detached hyaloids (32).

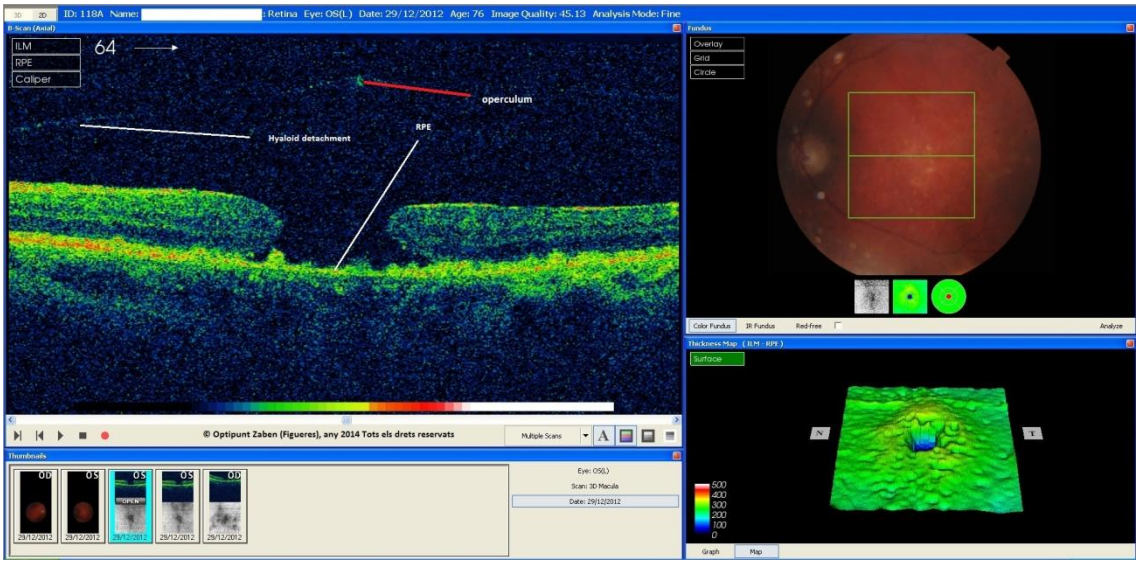

Figure 2.24. Full-thickness macular hole

A ***lamellar hole*** of the macula, which is caused by the effect of vitreal tractional force at the level of fovea, does not reach the photoreceptor layer (external retina) and, thus, visual acuity may be relatively good. The OCT image is asymmetric, in contrast with a macular hole.

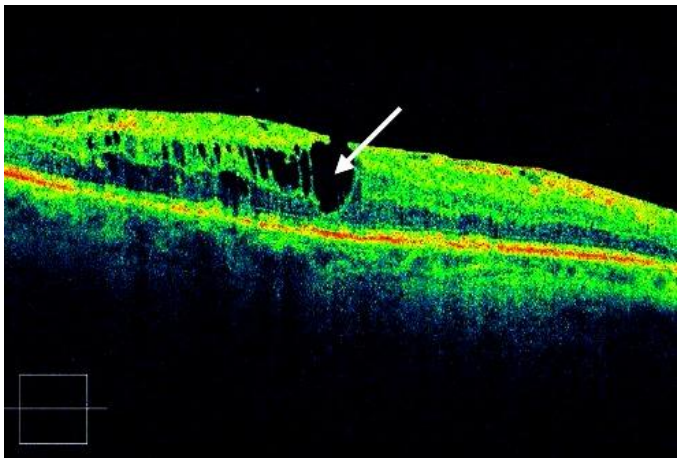

Figure 2.25. Lamellar macular hole (From: www.liv.ac.uk)

A ***pseudomacular hole*** is caused by the presence of an epiretinal membrane at the foveal level, causing alteration in the foveal contour. It is characterized by the smaller diameter of the fovea, symmetrical borders of the fovea, conservation of the foveal tissues and by its thickness (does not reach the outer retinal layers) (**Figure 2.26**).

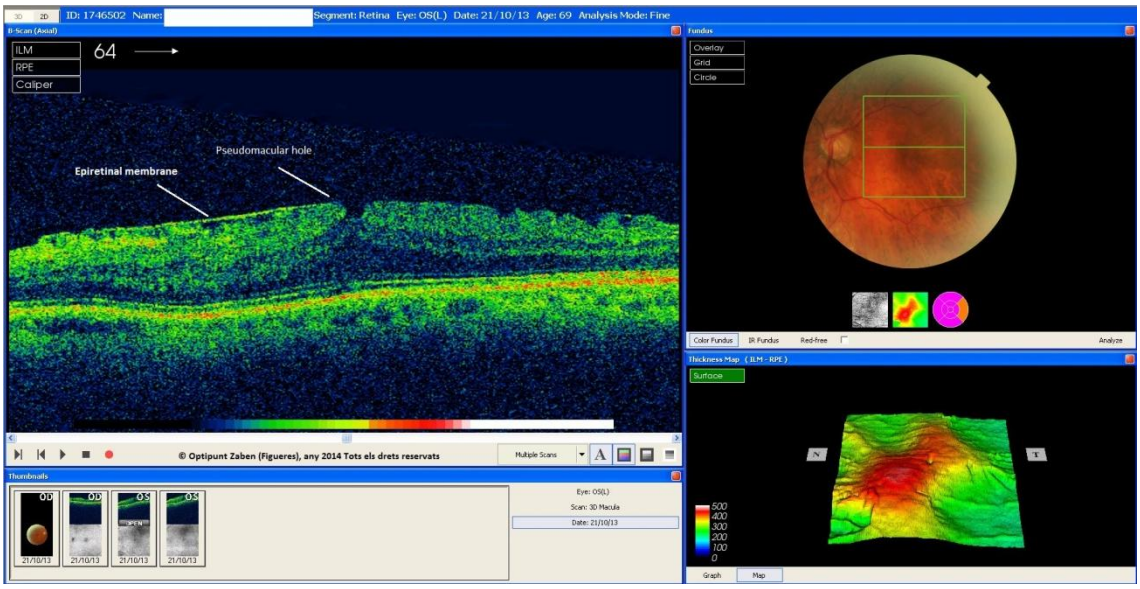

Figure 2.26. Pseudomacular hole

The ***Epiretinal membrane*** is a proliferation of the avascular fibrocellular tissue overlying the retinal surface associated with the condensation of the posterior hyaloids, pushing up the fovea and separating it from RPE, thus increasing the thickness of the pushed up area (**Figure 2.27**).

The appearance of an ***Age-related Macular Degeneration (ARMD)*** shows drusen, geographical atrophy of RPE, and choroidal neovascularisation (**Figure 2.28**). The OCT reveals the drusen as small elevated areas of RPE with the drusen seen below this layer, a condition known as pigmented epithelial detachment (PED) that is diagnosed in OCT when we see the red line (higher reflectivity) above the dim gaps (low reflectivity) of the drusen (33). The other associated type of retinal alterations, typical of wet ARMD (**Figure 2.29**), is neuroepithelium detachment (NED) seen by a red line (higher reflectivity) below the dim gap (low reflectivity). In addition, wet ARMD also

presents with intraretinal fluids, represented by gaps between the retinal layers with low reflectivity.

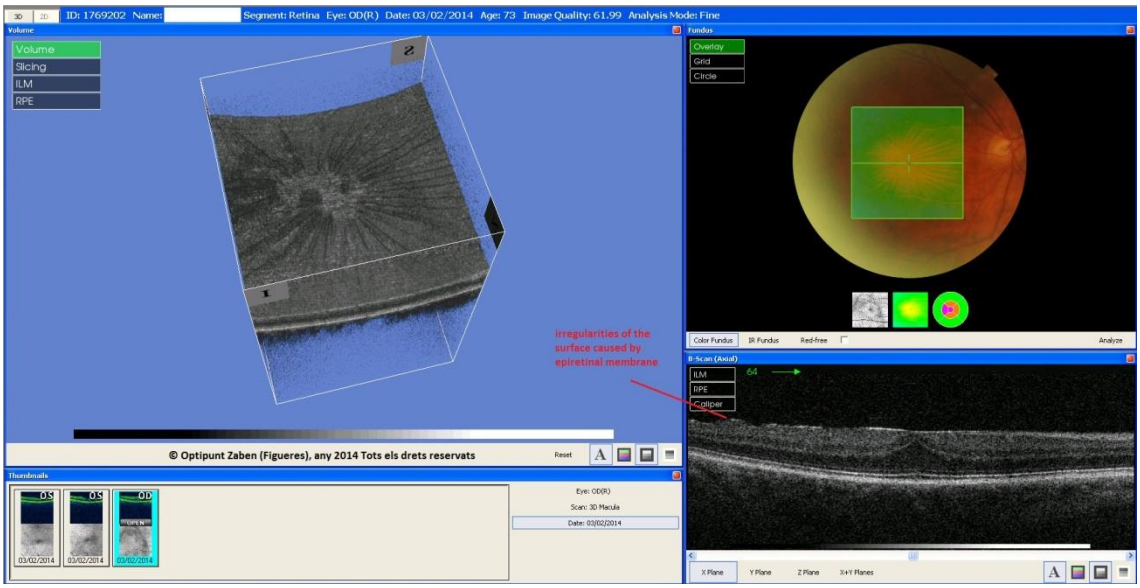

Figure 2.27. Epiretinal membrane

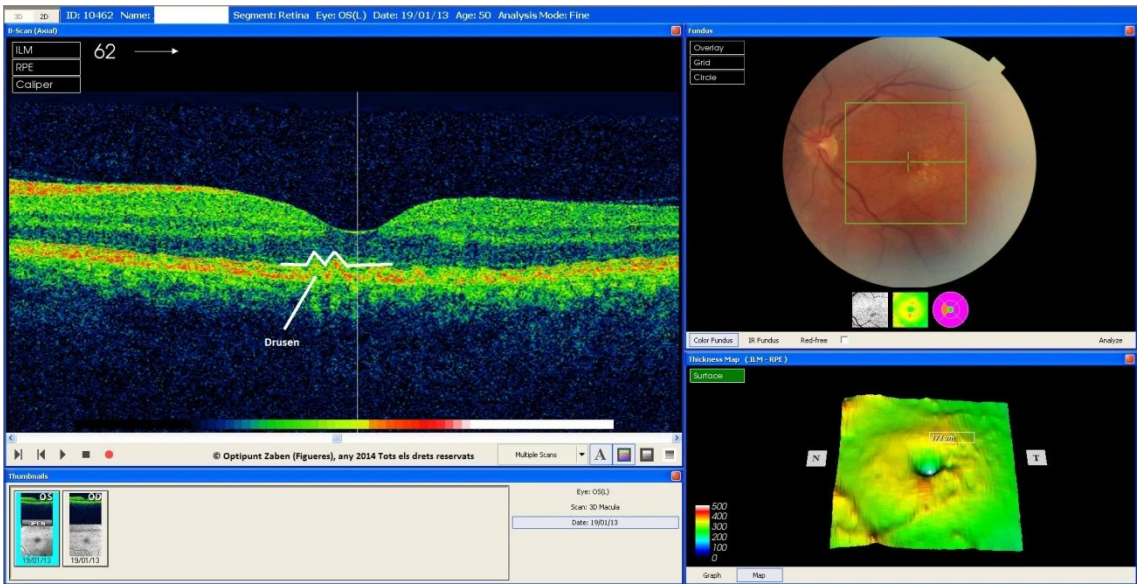

Figure 2.28. Early ARMD

In patients with ***diabetic retinopathy*** (34) OCT scan may help in identifying macular oedema and NED with lipid exudates (**Figure 2.30**). The retina is pushed up due to the effect of subretinal fluids causing an abnormal increase in thickness values.

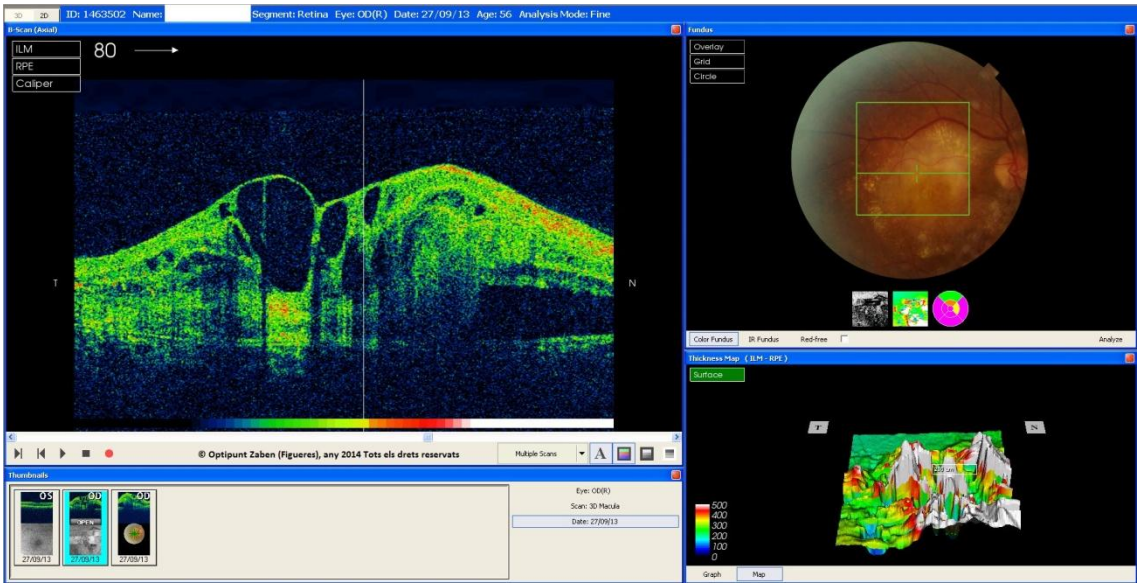

Figure 2.29. Wet exudative type of ARMD in the late stage

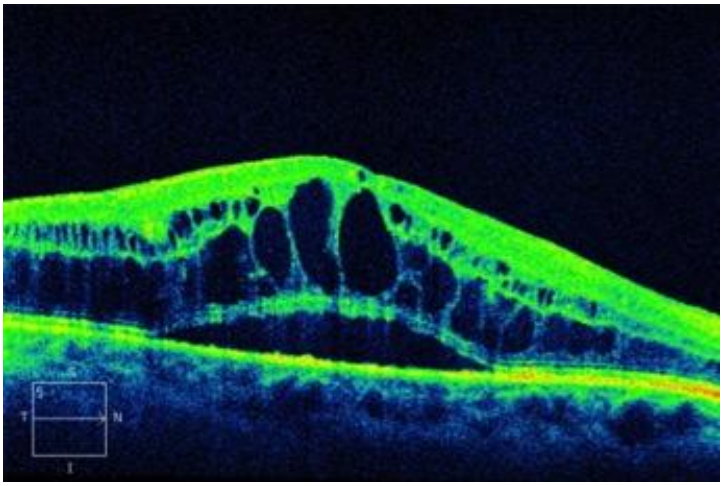

Figure 2.30. Macular Oedema in diabetic retinopathy (From: http://www.drbrendancronin.com.au/)

Central Serous Chorioretinopathy, a condition typically found in men (30-50 years of age) and associated to weight lifting or stress, is considered a self-limiting condition(35). It characterized by an idiopathic serious detachment of the neuroepithelium layer, seen as a red line (higher reflectivity) below the gap, and it could be accompanied by the presence of PED (the line above the gap) (**Figure 2.31**). There are abnormally large values in the scale of thickness as well.

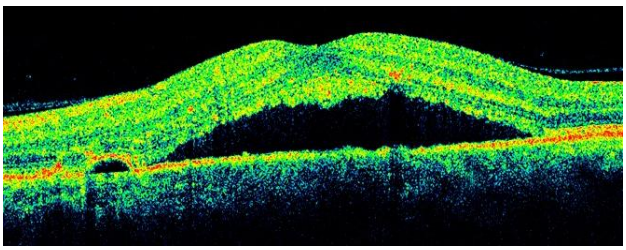

Figure 2.31. CSR (From: http://www.roescheisen.ch/)

Retinal Haemorrhage is a condition in which the retinal vessels are damaged due to an injury or certain diseases such as diabetes and arterial hypertension, temporary or permanently affecting vision (**Figure 2.32**). The retinal vessels consist in a dense network of small capillaries, in addition to the retinal vein and artery, are responsible to the retinal blood circulation.

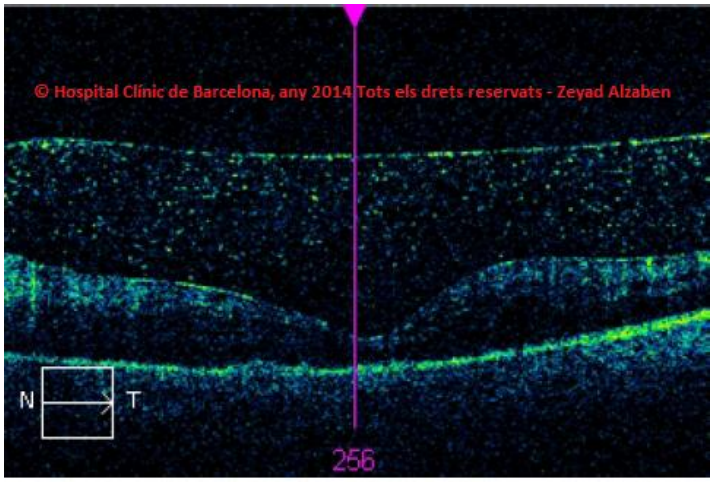

Figure 2.32. Retinal Haemorrhage at the level of macula

Finally, in ***high pathological myopia*** (36) we may observe an inclined image due to the effect of a posterior staphyloma (which is an sclera ectasia at the level of macula), and, in severe cases, retinal detachment. Also, there is increased reflectivity from the side of the choroid (in **Figure 2.33** it is more marked at the level of fovea) caused by RPE atrophy. Pathological myopia is characterized by extreme thinning of the retina.

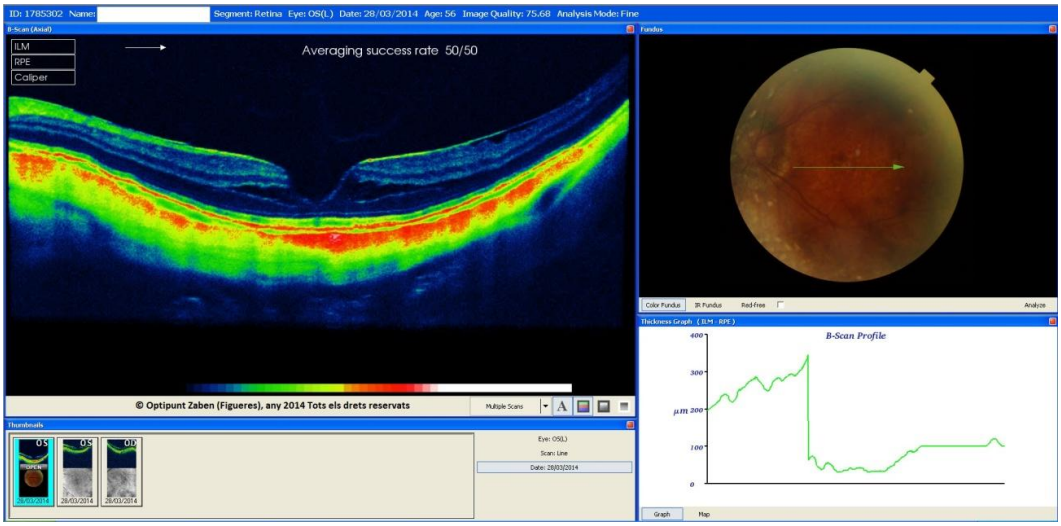

Figure 2.33. Left eye with pathological myopic macula

-Previous studies relevant to the present research

As was noted above, OCT is considered one of the most important devices for the objective and quantitative measurement of retinal structures. As such, this instrument is now included in most clinical protocols for the diagnosis and follow-up of glaucoma and optic nerve diseases. In these cases, it is very relevant to explore whether differences between the two eyes of the same patient are normal or whether this asymmetry may be considered an indicator of abnormality. (37)

Some of the previous studies using OCT scan to explore the retina are summarized in the following table:

Previous Studies (Year)	Study Type	Patients / Eyes	OCT Type
Park JJ et al. (2005) (38)		121 normal subjects	Stratus Model 3000
Sullivan-Mee M et al. (2013) (39)	Prospective cross-sectional cohort study	32 normal subjects and 40 primary open angle glaucoma subjects	Spectralis Heidelberg Engineering
Turk A et al. (2011) (40)	Observational case series	107 subjects / 107 eyes	Spectralis Heidelberg Engineering
Mwanza J C et al. (2010) (41)	Observational, clinical study	284 normal subjects / 568 eyes	Cirrus HD-OCT (Carl Zeiss Meditec, Inc)
Duan X R et al. (2010) (42)	Population-based cross-sectional study	2230 normal eyes	Stratus Model 3000
Altemir I et al. (2013) (43)	Prospective cross-sectional study	357 healthy children	Cirrus HD-OCT (Carl Zeiss Meditec, Inc)
Larsson E et al. (2011) (44)		56 normal children	Stratus Model 3000 and Spectralis Heidelberg Engineering
Budenz D L (2008) (45)		108 normal subjects	Stratus Model 3000
Huynh S C et al. (2006) (46)	Cross-sectional study	1765 children	Stratus Model 3000

Table 2.1. Previous studies related to OCT examination

In the experiment of Park and co-workers (38), the authors aimed at investigating the normal retinal asymmetry in terms of the thickness of the RNFL with respect to the horizontal and vertical line and also between the right and left eye. Park and colleagues defined normality as the absence of any ocular or systemic pathology that could alter the RNFL thickness, like diabetes mellitus, and as the best refractive correction providing a visual acuity better than 0.6. They reported a difference of C/D

of less than 0.2 in a fundus of C/D < 0.6 and concluded that the asymmetry between the right and left eye was insignificant for the superior and inferior quadrant and significant in the temporal and nasal quadrants (right RNFL thickness was higher than in the left eye). They also documented a correlation between the RNFL thickness and the refractive error for the inferior-nasal quadrants (thicker in hyperopic eyes).

Sullivan-Mee and colleagues (39) aimed at identifying the differences between 50 patients with primary early open-angle glaucoma, and 50 healthy patients (of normal IOP, visual field, and optic nerves) with normal open-angles by exploring the thickness of macula and the RNFL thickness of the superior and inferior quadrants. The authors concluded that the sensitivity of macular asymmetries to differentiate between normal and abnormal eyes was higher than for any other scanned area of the retina for subjects older than 40 years and in those with refractive errors of ≤5.00 D of sphere, and ≤3.00 D of cylinder, also considering the increased macular asymmetry and the decreased asymmetry of RNFL thickness of superior and inferior quadrants as an indicator of primary early open-angle glaucoma.

Turk's study (40) evaluated normal peripapillary RNFL thickness, macular volume and macular thickness in healthy eyes of Turkish children aged 6 to 16 years and with spherical equivalent of less than ±4.00 D. These authors revealed differences of ≤0.2 in C/D ratios in patients with C/D ratios ≤ 0.4 and also found thicker peripapillary RNFL in the superior and inferior quadrants, with the nasal quadrant being thinner than the temporal quadrant.

A similar study was conducted by Mwanza and co-workers (41) in 284 healthy adults (age > 18 years) of various ethnicities and C/D ≤ 0.5, with C/D differences of ≤0.2. The authors revealed average RNFL thickness differences of 0.52 microns, thicker in the right eye for the inferior, temporal, and nasal quadrants, whereas the superior quadrant was thicker in the left eye and concluded that more than 9 microns of RNFL thickness asymmetry could be indicative of early glaucoma.

The research group of Duan (42) evaluated normal macular thickness in adult Chinese healthy eyes and found mean values of 150.3 (±18.1 μm) for the foveal region, 176.4 (±17.5 μm) for the central region, 255.3 (±14.9 μm) for the inner region, and 237.7

(±12.4 µm) for the outer region. These authors found thinner values for the nasal quadrant than for the superior and inferior quadrants in the inner region of the macula and thicker values in the nasal quadrant in the outer region, also encountering overall greater values of macular thickness in men than in women.

Altemir and co-workers (43) evaluated RNFL thickness in a group of 357 healthy children aged 6 to 13 years and with spherical equivalent between -3.00 D +4.50 D and found higher values in the right temporal and nasal quadrants than the same quadrants in the left eye, and a thicker superior quadrant in the left eye than in the right eye. The authors considered the tolerance limits of intraocular difference for RNFL values to be 13.0 µm, and 23.2 µm for macular thickness.

Larsson's group research (44) also assessed the normal RNFL thickness asymmetry in a group of 56 healthy children (5-16 years old) with two different instruments: OCT and Heidelberg retina tomograph (HRT). They found mean RNFL thickness of 98.4 (SD 7.88 µm) using OCT, and 213.0 (SD 54.0 µm) using the HRT and presented tolerance limits of intraocular difference for between -9 to 9 µm using OCT and between -109 to 87 µm using HRT, that is, the OCT proved to offer less variability in RNFL thickness measurements than the HRT.

The study conducted by Bundez (45) also explored normal RNFL thickness symmetry in 108 subjects aged between 20 and 82 years, with a large spherical equivalent range (+4.50 to -7.50 D). This author found thicker right eye RNFL values by 1.3 µm and defined tolerance limits of intraocular differences in RNFL within the range of -10.8 to +8.9 µm, never exceeding more than 9 to 12 µm.

Finally, the research of Huynh and colleagues (46) was aimed to assess the normal retinal symmetry of macular, peripapillary, and papillary RNFL thickness in young children. The authors revealed that 95% of subjects had intraocular differences of <22 µm for minimal foveal thickness, and <40 µm for other areas.

In summary, the OCT has been used to explore asymmetries. In the present study the Topcon 3D OCT-2000 will be used to explore physiological asymmetries in healthy young adult European-Caucasian subjects (age range from 12 to 23 years old and

spherical equivalent range from -3.00 to +4.00 D). The average RNFL thickness, 4 quadrants RNFL thickness, central macular thickness, macular volume, average macular thickness, rim area thickness, disc area thickness and C/D ratio shall be explored, and the association between the various parameters investigated.

3. Objectives and Hypothesis

3.1. General objectives

The main objective of the present research was to establish a diagnostic clinical method using the scanning protocol of the OCT for the optic nerve head (ONH) and the retinal nerve fibre layer (RNFL), as well as the macular area, to examine the physiological asymmetry between the right and the left eye in a sample of young adults aged between 12 and 23 years and with an spherical equivalent ranging from -3.00 to +4.00 dioptres.

3.2. Specific objectives

To investigate the importance of the OCT for the clinical management in optometry while emphasizing the importance of knowing the asymmetrical normal range of retinal parameters as a physiological reference for the clinical management and diagnosis of certain unilateral or asymmetrical ocular pathologies.

3.3. Hypothesis

“There is a normal range of asymmetry in the diverse retinal physiological parameters measured using optical coherence tomography (3D OCT - 2000) in a group of young adults (12 - 23 years old) that may be used as a new method for evaluating certain ocular pathologies”.

4. Experimental method

4.1. Study sample

The study was conducted between April 2014 and June 2014. Patients were recruited from those attending a busy optometric clinic (Optipunt Zaben, Figueres) for routine visual examination. The following inclusion/exclusion criteria were defined:

- Inclusion criteria are young adult patients aged from 12 to 23 years, with spherical equivalent within the range of +4.00 D to -3.00 D.
- Exclusion criteria are any pathology that could alter the macular area, patients without central fixation and patients with significant anisometropia.

All patients were informed of the purpose of the study (parents were informed if patients were underage) and were given written information, whereupon they signed an informed consent (see **Annex I**). The study was conducted in accord with the Declaration of Helsinki tenets of 1975 (as revised in Tokyo in 2004).

4.2. Instruments and equipment

For the purpose of this study, the typical instrumentation found in an optometric practice was employed for routine visual examination. This included retinoscope, CV.5000 Digital phoropter (Topcon), digital slit-lamp biomicroscope (Topcon), air-puff tonometer (Topcon KR.1) and KR.1 Auto Kerato Refractometre (Topcon). In addition, the following equipment was used for retinal and visual acuity measurements:

- 3D OCT.2000 Optical Coherence Tomography – Topcon
- Logarithmic Visual Acuity Chart "ETDRS (Early Treatment Diabetic Retinopathy Study)" with notations for testing at 4 meters (13 feet) Chart "1" – Precision Vision ™

4.3. Procedure

A clinical prospective and transversal study was designed. During the first visit a general optometric and ophthalmological case history was compiled including information on name, sex, date of birth (age), general diseases (diabetes mellitus, hypertension, cardiovascular diseases, etc.), familiar background of glaucoma, history of frequent headaches, previous or actual systemic treatment (corticosteroids, etc.). Then, a complete optometric exploration was performed to determine whether the patient was a candidate for the study according to the inclusion/exclusion criteria described above. Non-dilated pupil examination in normal environmental conditions was conducted to determine refractive error.

Best corrected visual acuity was measured with the ETDRS test, which is a retro-illuminated box of 62.9 cm X 65.4 cm X 17.8 cm (Lighthouse International) presented at a distance of 4 meters and allows for logMAR notation (logarithm of the minimum angle of resolution).

Also, the health of the ocular structures was explored with a slit-lamp examination in which we observed the eyelids, sclera, conjunctiva, cornea, tear film, crystalline lens, and in general the anterior segment of the eye, with the objective of evaluating the ocular media, highlighting any ocular pathology of the anterior segment.

Finally, intraocular pressure was evaluated with an air-puff tonometer (Topcon KR 1) without any direct contact with the ocular surface.

4.4. Optic Coherence Tomography

All patients were then studied to establish normal values of thickness and macular volume obtained with a SD-OCT, using the cube 512 × 128 macular protocol for 3D-OCT-2000. All OCT measurements were performed by the same examiner.

The macular cube 512 × 128 protocol (**Figure 4.1**) performs 512 cuts of horizontal B-scans with 128 A-scans per cut over an area of 6 × 6 mm, offering a thickness map with concentric sectors defining the nine regions of the macular map. The average thickness

of all points within the inner circle of 1 mm diameter is defined as the central retinal thickness (central subfield thickness).

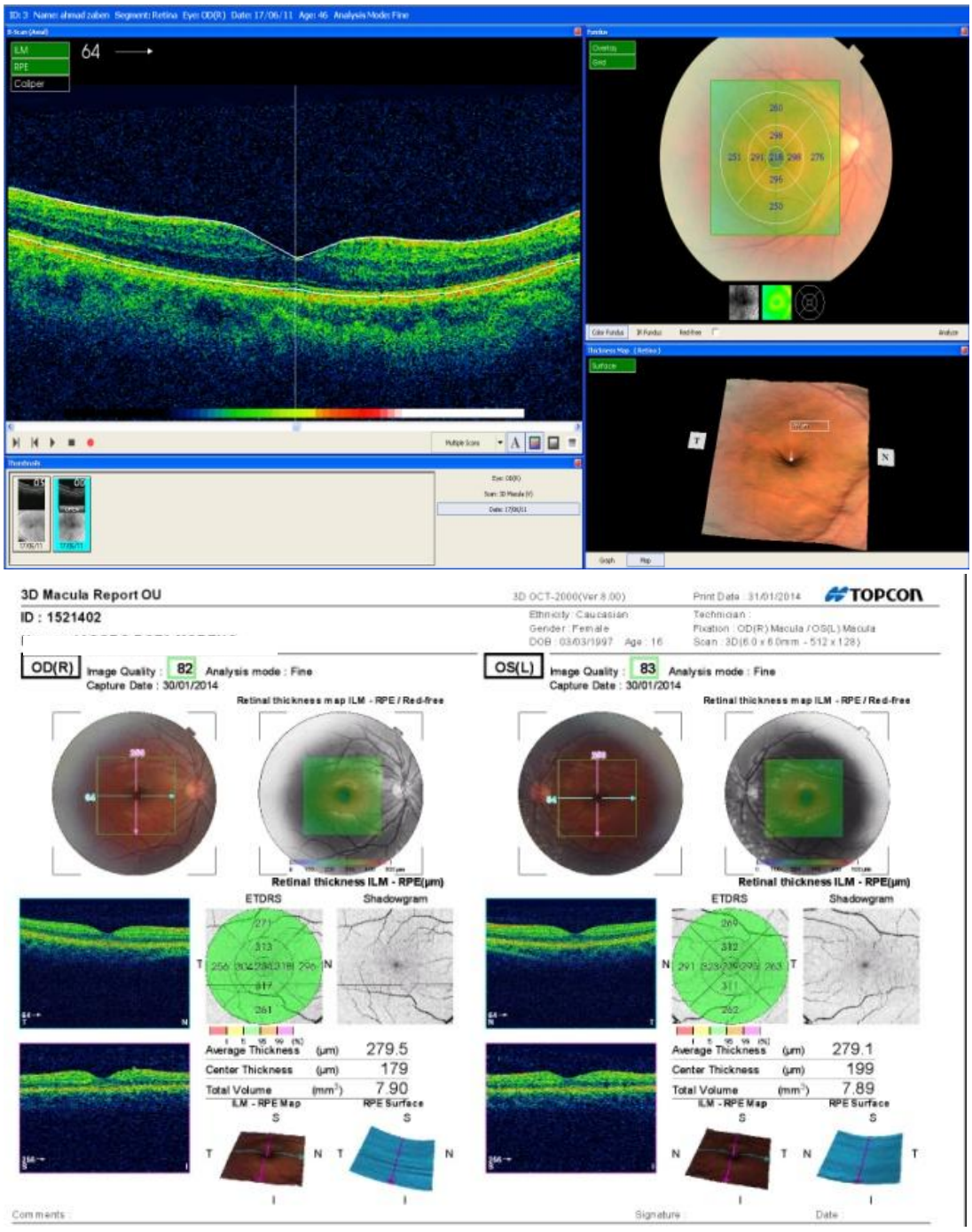

Figure 4.1. OCT scan of the macula and its corresponding results

The volume cub and cub average thickness are generated by internal algorithms of 3D-OCT-2000. In our study, the macular cub protocol was considered normal if:

a) It showed no retinal changes.

b) The signal strength was greater than 70%.

c) It was properly centred on the fovea.

The optic disc cub of 512 X 128 protocol was then employed (**Figure 4.2**). The scan was adjusted to the size of the optic disc as close as possible to the disc margin without crossing the border of optic nerve at any point.

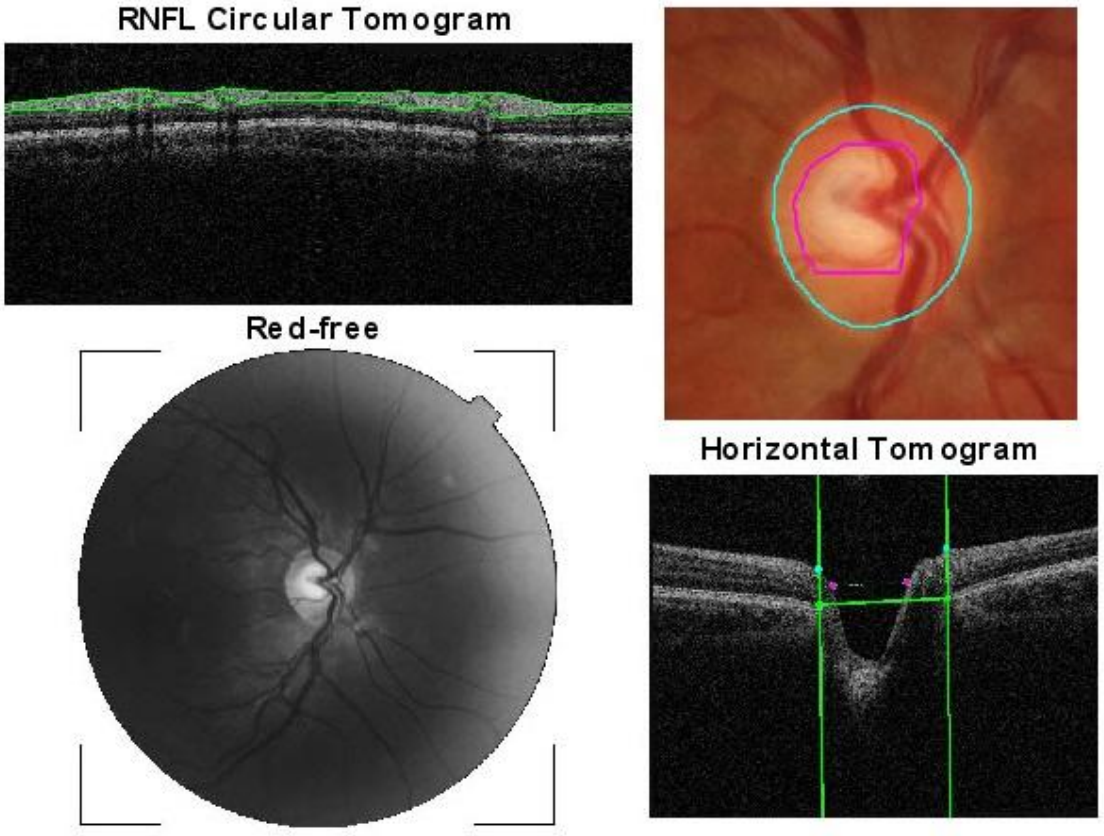

Figure 4.2. OCT scan of the optic nerve showing the C/D ratio

In **Figure 4.2** the cup (inner pink circle) is automatically detected and drawn by the OCT software (Version 8.00). The region between the disc (green line) and the cup margins is the neuroretinal rim area (mm^2), whereas the cup area (mm^2) corresponds to the

region inside the cup margin. The summation of these areas is the disc area (mm^2), and the square root of the ratio of cub to disc areas determines the C/D ratio (see **Figure 4.3**).

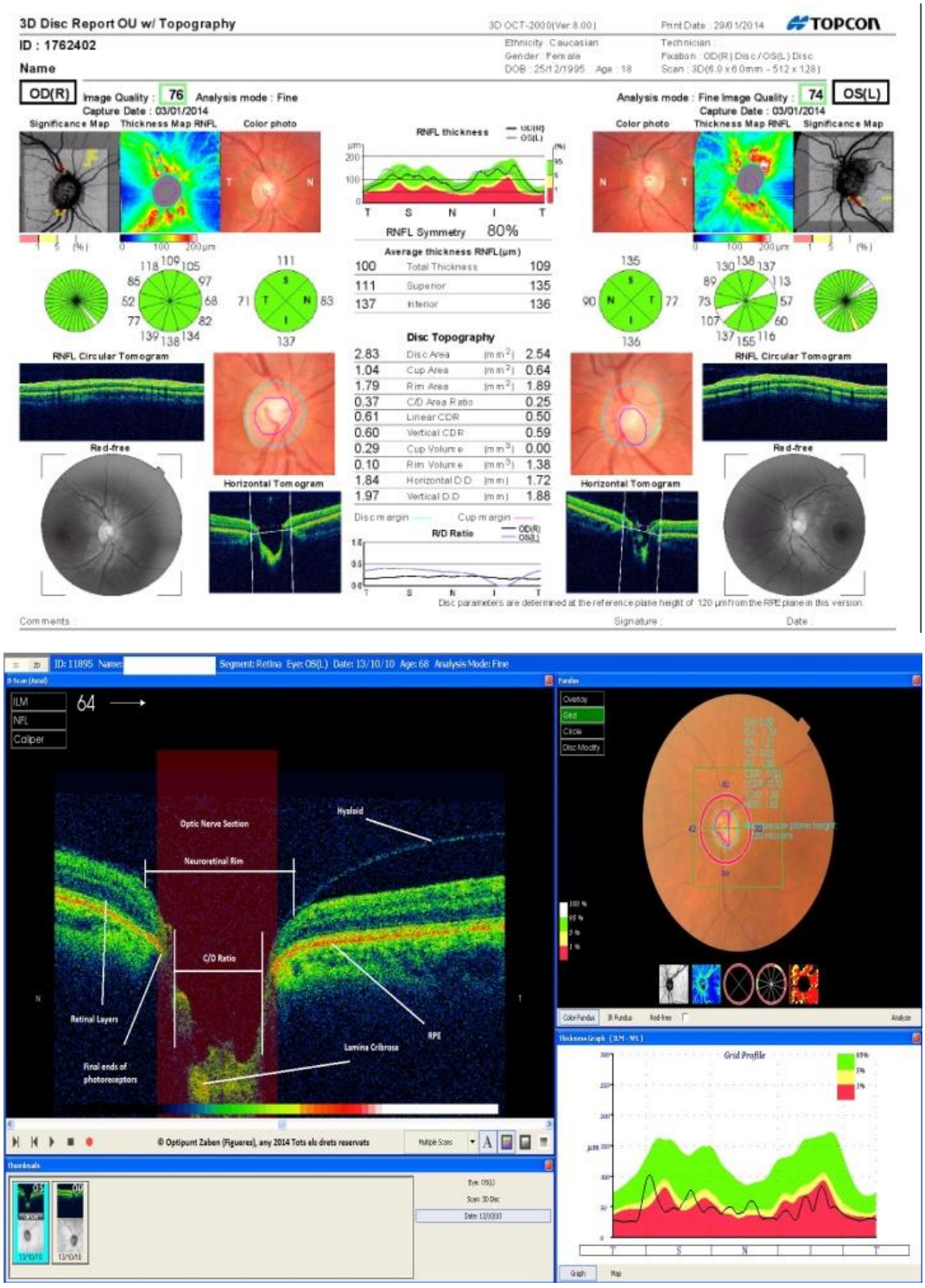

Figure 4.3. OCT scan of the optic nerve head and its corresponding results

Measurements of RNFL thickness were obtained using the automated software measurement analysis protocol of RNFL thickness (single eye).

During image acquisition, the image quality is a very important issue. To accept scans, in addition to their good quality in terms of integrity and optimized polarization, the centralization around the optic disc was also observed. No scans were accepted if there were signs of eye movement, blinking, or not considered (by the examiner) as properly centred.

The following table offers a summary of the parameters used in the present study.

Parameter	Name	Function
DA	Disc Area (mm^2)	Area of the region surrounded by a yellow line
RA	Rim Area (mm^2)	Area of the region between the above mentioned two lines
CDR	Cup Disc Ratio	Ratio of area cup/disc

Table 4.2. Retinal and optic disc parameters explored in the present study

4.5. Statistical Analysis

All statistical analyzes were performed using SPSS software (IBM, Inc.) version 17.00 for Windows 7. Before conducting the statistical analysis we examined our data for normality with the Kolmogorov-Smirnov test, revealing several instances of non-normal distribution. Therefore, we opted to present our results for each eye, as well as the differences between eyes, as median and range (minimum and maximum), although mean values and standard deviation (±SD) are also summarized to allow comparison with previous studies. In order to explore the statistical significance of the differences between non-paired data (such as between males and females) the Mann-

Whitney U-test was used, whereas when data was paired (comparing right with left eye), the Wilcoxon signed ranks test was used. Finally, the Spearman correlation test was employed to explore possible associations between the variables under evaluation. For this test, and given the clinical nature of the present study, we considered a rho coefficient ≥ ±0.4 as an indicator of either a positive or negative weak correlation between variables, a rho value between 0.6 and 0.8 as an indicator of moderate correlation and any rho ≥±0.8 as an indicator of strong correlation. A p value <0.05 denoted statistical significance throughout the study.

5. Results and Discussion

5.1. Study sample description

After the exclusion of 11 subjects who did not comply with the inclusion and exclusion criteria or who presented insufficiently clear retinal fundus images, a total of 37 subjects (n = 37) participated in this research, *i.e.*, 74 eyes. 14 subjects were male (age range: 13 – 23 years old) and 23 were female (12-23 years old).

Table 5.1 presents a summary of visual acuity (in logMAR) and refractive status data for the present study sample in terms of right eye (OD) and left eye (OS)

Parameter	Mean	SD	Median	Maximum	Minimum
VA (logMAR) OD	0.025	0.041	0.000	0.160	0.000
VA (logMAR) OS	0.021	0.040	0.000	0.160	0.000
Spherical Equivalent OD (D)	-1.33	1.30	-1.00	0.50	-3.75
Spherical Equivalent OS (D)	-1.23	1.41	-1.00	1.00	-3.75

Table 5.1. Visual acuity and refractive status descriptive statistics

5.2. Retinal parameters under study

Table 5.2 offers a summary of all the data recorded with the OCT for both eyes.

Turk's study (40) described thicker peripapillary RNFL in the superior and inferior quadrants, with the nasal quadrant being thinner than the temporal quadrant. In the present study, peripapillary thickness was found to show a different pattern, with values for the right eye decreasing from the inferior (mean =130.18 μm) to the superior (mean = 124.05 μm), nasal (mean =82.08 μm), and temporal (mean = 74.75 μm) quadrants, and for the left eye decreasing from the inferior (mean =132.7568) to the superior (mean = 128.40 μm), nasal (mean =82.72 μm), and temporal (mean = 74.21 μm) quadrants. It must be mentioned that our age range was different from that of Turk's study (12 to 23 years instead of 6 to 16 years). Disagreement between studies is not uncommon in the literature, however. For example, Duan's research group (42) found thicker values for the nasal quadrant than for the superior and inferior quadrants.

Parameter	Mean	SD	Median	Maximum	Minimum
Mean RNFL thick OD (μm)	102.81	7.39	102.00	122.00	92.00
Mean RNFL thick OS (μm)	104.51	7.36	104.00	123.00	91.00
SQ RNFL thick OD (μm)	124.05	11.61	125.00	146.00	102.00
SQ RNFL thick OS (μm)	128.40	11.89	130.00	149.00	105.00
IQ RNFL thick OD (μm)	130.18	12.97	134.00	163.00	110.00
IQ RNFL thick OS (μm)	132.75	12.86	135.00	158.00	108.00
NQ RNFL thick OD (μm)	82.081	12.98	84.00	108.00	60.00
NQ RNFL thick OS (μm)	82.72	14.40	80.00	121.00	60.00
TQ RNFL thick OD (μm)	74.75	6.62	75.00	87.00	58.00
TQ RNFL thick OS (μm)	74.21	8.94	73.00	96.00	60.00
Rim area OD (mm^2)	1.88	0.34	1.89	2.64	1.18
Rim area OS (mm^2)	1.92	0.37	1.93	2.72	1.25
Disc area OD (mm^2)	2.45	0.43	2.49	3.52	1.68
Disc area OS (mm^2)	2.48	0.56	2.47	3.72	0.12
CD ratio OD	0.22	0.11	0.21	0.46	0.05
CD ratio OS	0.24	0.13	0.24	0.54	0.02
Central macular thick OD (μm)	195.54	27.66	183.00	310.00	169.00
Central macular thick OS (μm)	208.94	33.98	200.00	314.00	171.00
Macular Vol OD (mm^3)	7.75	0.33	7.72	8.52	7.17
Macular Vol OS (mm^3)	7.75	0.36	7.75	8.60	7.17
Mean macular thick OD (μm)	274.21	12.00	273.50	301.40	253.60
Mean macular thick OS (μm)	274.35	12.98	274.20	304.20	253.50

Table 5.2. Descriptive statistics of all retinal OCT parameters

For our data analysis, firstly, we explored whether there were differences in any parameter between males and females, using the Mann-Whitney U - test, which is the non-parametric equivalent for the Student's t-test when the data are not paired. We considered a p-value <0.05 to be statistically significant, and z-value >1.96 as a predetermined significance level.

	Male					**Female**						
	Mean	SD	Median	Maximum	Minimum	Mean	SD	Median	Maximum	Minimum	**z-value**	**p-value**
Age (years)	18.86	3.06	19.00	23	13	16.09	3.42	15.00	23	12	-2.347	**0.018**
Mean RNFL OD (μm)	105.92	4.06	106.00	113.00	99.00	100.91	8.35	99.00	122.00	92.00	-2.306	**0.020**

Table 5.3. The Mann-Whitney U-test and Descriptive statistics for age and Mean RNFL OD

The statistical analysis (**Table 5.3**) revealed significant differences only in age and mean thickness of RNFL in the right eye between males and females. This is an unexpected result, previously unreported in the literature, which would require further study with a large study sample with better gender distribution. It must be noted that Duan's research group (42) revealed differences between males and females in mean macular thickness, which we failed to discover from our data analysis.

Next, we assessed the differences between the right eye and the left eye for the same subjects using the Wilcoxon signed ranks test, which is the non-parametric equivalent of the Student's t-test for paired samples (**Table 5.4**). We considered p-value <0.05 to be statistically significant, and z-value >1.96 as a predetermined significance level.

Parameter	Mean	SD	Median	Maximum	Minimum	z-value	p-value
VA (logMAR) dif	-0.02	0.16	0.00	0.10	-1.00	-1.342	0.180
Spherical Equiv (D) dif	-0.10	0.37	0.00	0.50	-1.00	-1.297	0.195
Mean RNFL thick dif (μm)	-1.70	3.23	-1.00	6.00	-9.00	-2.959	**0.003**
SQ RNFL thick dif (μm)	-4.35	8.73	-4.00	9.00	-28.00	-2.658	**0.008**
IQ RNFL thick dif (μm)	-2.56	8.56	-2.00	14.00	-25.00	-1.528	0.126
NQ RNFL thick dif (μm)	-0.64	9.72	-2.00	18.00	-20.00	-0.340	0.734
TQ RNFL thick dif (μm)	0.54	5.47	2.00	12.00	-13.00	-0.961	0.337
Rim area dif (mm^2)	-0.04	0.26	-0.04	0.35	-1.01	-0.664	0.507
Disc area dif (mm^2)	-0.03	0.46	-0.09	2.07	-1.20	-1.430	0.153
CD ratio dif	-0.02	0.09	-0.02	0.12	-0.28	-1.318	0.187
Central macular thick dif (μm)	-13.40	27.86	-10.00	31.00	-81.00	-2.640	**0.008**
Macular Vol dif (mm^3)	-0.00	0.14	0.00	0.46	-0.33	-0.574	0.566
Mean macular thick dif (μm)	-0.13	5.22	0.00	16.10	-11.80	-0.558	0.577

Table 5.4. Descriptive statistics and Wilcoxon signed ranks test for differences between both eyes (right eye minus left eye values). Statistically significant differences are shown in bold

No statistically significant inter-ocular differences were found in either logMAR visual acuity or spherical equivalent. This finding is of relevance, as both eyes needed to be as similar as possible in order to explore "normal" ocular asymmetry.

Only three retinal parameters were found to present statistically significant differences between fellow eyes: mean RNFL thickness, superior quadrant RNFL thickness and central macular thickness. These findings are in disagreement with the study of Park and co-workers (38), in which the authors failed to find any statistically significant difference between the two eyes for the superior and inferior quadrant but disclosed

significant differences for the temporal and nasal quadrants (RNFL thickness was higher in the right eye than in the left eye).

Sullivan-Mee and colleagues (39) described a decreased asymmetry in superior and inferior quadrant RNFL thickness as a possible indicator of early primary open-angle glaucoma, although their study explored patients older than 40 years, that is, they documented the increased value of the difference between the two eyes for those quadrants in normal eyes. In agreement with that research, our findings with young healthy subjects revealed greater asymmetries in the inferior (mean = -2.56 μm) and superior (mean = -4.35 μm) quadrants.

Mwanza and co-workers (41) assumed that the normal difference in adults (age > 18 years) in average RNFL thickness was 0.52 μm, thicker in the right eye for the inferior, temporal, and nasal quadrants, whereas the superior quadrant was thicker in the left eye. These authors noted that any value exceeding 9 μm could be indicative of early glaucoma, which was the same tolerance limit defined by Larsson's group (44), although Bundez (45), in a study in adults aged between 20 and 82 and with a larger range of refractive errors, set 12 μm as the maximum safe inter-ocular difference in RNFL thickness. Similar results were found by Altemir and co-workers (43) in a group of healthy children aged 6 to 13 years and with spherical equivalent between -3.00 D +4.50 D. These authors reported higher values in the right eye than in the left eye for temporal and nasal quadrants, and a thicker superior quadrant in the left eye than in the right eye. In contrast, in our study we encountered a much smaller normal difference between both eyes in average RNFL thickness (-1.70 μm), and disclosed the left eye to be thicker than the right eye for the superior, inferior, and nasal quadrants, whereas the temporal quadrant was thicker in the right eye.

Finally, the research of Huynh and colleagues (46), in which normal retinal symmetry of macular, peripapillary, and papillary RNFL thickness was assessed in a group of young children, revealed that 95% of subjects had intraocular differences of <22 μm for minimal foveal thickness, and <40 μm for other areas.

5.3. Correlation analysis

In agreement with the study of Park and co-workers, as shown in **Table 5.5**, our analysis with the Spearman's rho correlation test revealed the same statistically significant although weak correlations between refractive power (in spherical equivalent) and RNFL thickness for the inferior and nasal quadrants (it must be noted that the correlation between spherical refraction and IQ RNFL thickness for the right eye is below 0.4, that is, this result may not be interpreted as a correlation but only as a certain trend between the two variables).

Parameters	**IQ RNFL thick OD (µm)**		**NQ RNFL thick OD (µm)**	
SE (D) OD	rho	p-value	rho	p-value
	0.352	**0.033**	0.453	**0.005**
Parameters	**IQ RNFL thick OS (µm)**		**NQ RNFL thick OS (µm)**	
SE (D) OS	rho	p-value	rho	p-value
	0.421	**0.010**	0.514	**0.001**

Table 5.5. Correlations between spherical equivalent (SE) and RNFL for inferior and nasal quadrants and both eyes

In addition, our data analysis revealed statistically significant correlations between macular volume in the right eye and all the other retinal parameters, with the exception of RNFL thickness in the temporal quadrant and central macular thickness (**Table 5.6**). For the left eye, statistically significant correlations were unveiled between macular volume and all the other retinal parameters with the exception of superior and temporal quadrant RNFL thickness and also central macular thickness (**Table 5.7**).

Parameters	**Macular Vol OD (mm^3)**	
	rho	p-value
SE (D) OD	0.450	**0.005**
Mean RNFL thick OD (µm)	0.584	**<0.001**
IQ RNFL thick OD (µm)	0.418	**0.010**
SQ RNFL thick OD (µm)	0.451	**0.005**
NQ RNFL thick OD (µm)	0.547	**<0.001**
TQ RNFL thick OD (µm)	-0.090	0.596
Mean macular thick OD (µm)	0.999	**<0.001**
Central macular thick OD (µm)	0.202	0.231

Table 5.6. Correlations between the macular volume and other parameter in OD. Statistically significant differences are shown in bold

Parameters	Macular Vol OS (mm^3)	
	rho	p-value
SE (D) OS	0.391	**0.017**
Mean RNFL thick OS (μm)	0.468	**0.003**
IQ RNFL thick OS (μm)	0.394	**0.016**
SQ RNFL thick OS (μm)	0.044	0.798
NQ RNFL thick OS (μm)	0.576	**<0.001**
TQ RNFL thick OS (μm)	0.011	0.946
Mean macular thick OS (μm)	1.000	**<0.001**
Central macular thick OS (μm)	0.152	0.370

Table5.7. Correlations between the macular volume and other parameter in OS. Statistically significant differences are shown in bold

The difference in macular volume between the two eyes in our sample was not found to be correlated with any other difference in retinal parameters. This finding is relevant, as any correlation could be an indication of a retinal pathological condition.

Parameters	Macular Vol dif (mm^3)	
	rho	p-value
SE (D) dif	-0.122	0.472
Mean RNFL thick dif (μm)	0.064	0.708
IQ RNFL thick dif (μm)	0.143	0.399
SQ RNFL thick dif (μm)	-0.015	0.931
NQ RNFL thick dif (μm)	0.117	0.491
TQ RNFL thick dif (μm)	-0.173	0.305
Mean macular thick dif (μm)	-0.148	0.383
Central macular thick dif (μm)	0.156	0.358

Table 5.8. Correlations between the macular volume and other parameter in both eyes. There are no statistically significant differences.

6. Conclusions

The main conclusions of the present study may be summarized as follows:

- Using OCT (3D-OCT 2000 Topcon) to explore the physiological asymmetries of the retina among normal adults is an effective approach to predict any suspected pathology of the retina such as early glaucoma.

- Statically significant differences were found between males and females in mean thickness of RNFL in the right eye.

- Eyes from our study sample could be considered similar, as no inter-ocular differences in visual acuity or spherical equivalent were found. Therefore, normal retinal asymmetry values could be safely explored.

- The inferior quadrant was found to be thicker than the other quadrants in both eyes.

- Inter-ocular statistically significant differences were uncovered in mean RNFL thickness, superior quadrant RNFL thickness and central macular thickness. Mean RNFL thickness for the left eye was higher than for the right eye by 1.70 μm.

- There was correlation between refractive power and RNFL thickness in the inferior and nasal quadrants.

- Macular volume did not correlate with central macular thickness in any eye. Any correlation between the differences of the macular volume of the two eyes and the differences of the other parameters could be an indication of pathological condition of the retina.

7. Limitations and future prospects

This study may present some limitations, the main one is the difficulty to compare its findings with those of previous researches, as both the instrumentation and the age range were very different. Similarly, another limitation is related to the race of the subjects enrolled in the study, as only the European-Caucasian participants were included, and thus our findings may not be applicable to other racial categories. Therefore, we believe that future studies with a larger sample size are required to confirm our findings.

8. References

1. Welfer D, Scharcanski J, Marinho DR. Fovea center detection based on the retina anatomy and mathematical morphology. Comput Methods Programs Biomed. 2011 Dec;104(3):397–409.

2. Hildebrand G, Fielder A, Reynolds J, Olitsky. Anatomy and physiology of the retina. In: Pediatric Retina [Internet]. Berlin Heidelberg: Springer-Verlag; 2011. 39-65 p.

3. Wenner Y, Wismann S, Preising MN, Jäger M, Pons-Kühnemann J, Lorenz B. Normative values of peripheral retinal thickness measured with Spectralis OCT in healthy young adults. Graefes Arch Clin Exp Ophthalmol Albrecht Von Graefes Arch Klin Exp Ophthalmol. 2014 Feb 11.

4. Kumar J, Paul SD, Singh K. Periphery of the retina. A clinical study. Ophthalmol J Int Ophtalmol Int J Ophthalmol Z Für Augenheilkd. 1971;163(3):150–170.

5. Vidya SA, Balasubramanian S, Chandrasekaran V. Automatic Detection of Anatomical Structures in Digital Fundus Retinal Images. Conf Mach Vis Appl. 2007 May 16;13:483–486.

6. Youssif AR, Ghalwash AZ, Ghoneim AR. Optic disc detection from normalized digital fundus images by means of a vessels' direction matched filter. IEEE Trans Med Imaging. 2008 Jan;27(1):11–18.

7. Jaffe GJ, Caprioli J. Optical coherence tomography to detect and manage retinal disease and glaucoma. Am J Ophthalmol. 2004 Jan;137(1):156–169.

8. Hoffmann EM, Zangwill LM, Crowston JG, Weinreb RN. Optic Disk Size and Glaucoma. Surv Ophthalmol. 2007;52(1):32–49.

9. Friedman DS, O'Colmain BJ, Muñoz B, Tomany SC, McCarty C, de Jong PTVM, et al. Prevalence of age-related macular degeneration in the United States. Arch Ophthalmol. 2004 Apr;122(4):564–572.

10. Chan A, Duker JS, Schuman JS, Fujimoto JG. Stage 0 Macular Holes: Observations by Optical Coherence Tomography. Ophthalmology. 2004 Nov;111(11):2027–2032.

11. Gardlik R, Fusekova I. Pharmacologic Therapy for Diabetic Retinopathy. Semin Ophthalmol. 2014 Feb 27.

12. Chan A, Duker JS, Ko TH, Fujimoto JG, Schuman JS. Normal Macular Thickness Measurements in Healthy Eyes Using Stratus Optical Coherence Tomography. Arch Ophthalmol. 2006 Feb;124(2):193–198.

13. Alkin Z, Ozkaya A, Osmanbasoglu OA, Agca A, Karakucuk Y, Yazici AT, et al. The role of epiretinal membrane on treatment of neovascular age-related macular degeneration with intravitreal bevacizumab. ScientificWorldJournal. 2013 Dec 24;2013:958724.

14. Bouzas EA, Karadimas P, Pournaras CJ. Central Serous Chorioretinopathy and Glucocorticoids. Surv Ophthalmol. 2002 Sep;47(5):431–448.

15. Mandal N, Harborne P, Bradley S, Salmon N, Holder R, Denniston AK, et al. Comparison of two ophthalmoscopes for direct ophthalmoscopy. Clin Experiment Ophthalmol. 2011 Jan;39(1):30–36.

16. Petrushkin H, Barsam A, Mavrakakis M, Parfitt A, Jaye P. Optic disc assessment in the emergency department: a comparative study between the PanOptic and direct ophthalmoscopes. Emerg Med J EMJ. 2012 Dec;29(12):1007–1008.

17. Leitritz MA, Oltrup T, Umesh Babu H, Bende T, Bartz-Schmidt KU, Foerster MH. [Improvement of power and illumination source of the indirect binocular ophthalmoscope designed by Foerster]. Klin Monatsblätter Für Augenheilkd. 2013 Aug;230(8):825–828.

18. Winters JE, Frantz KA, Kern RM. Accommodative and vergence difficulties interfering with image clarity through a binocular indirect ophthalmoscope. Optom Vis Sci Off Publ Am Acad Optom. 2004 Apr;81(4):260–267.

19. Harle DE, Davies K, Shah R, Hussain S, Cowling S, Panesar TK, et al. Technical Note: A comparison of a novel direct ophthalmoscope, the Optyse, to conventional direct ophthalmoscopes. Ophthalmic Physiol Opt J Br Coll Ophthalmic Opt Optom. 2007 Jan;27(1):100–105.

20. Mark HH. On the evolution of binocular ophthalmoscopy. Arch Ophthalmol. 2007 Jun;125(6):830–833.

21. Conrath J, Giorgi R, Raccah D, Ridings B. Foveal avascular zone in diabetic retinopathy: quantitative vs qualitative assessment. Eye Lond Engl. 2005 Mar;19(3):322–326.

22. Nouri-Mahdavi K, Hoffman D, Tannenbaum DP, Law SK, Caprioli J. Identifying early glaucoma with optical coherence tomography. Am J Ophthalmol. 2004 Feb;137(2):228–235.

23. Ehnes A, Wenner Y, Friedburg C, Preising MN, Bowl W, Sekundo W, et al. Optical Coherence Tomography (OCT) Device Independent Intraretinal Layer Segmentation. Transl Vis Sci Technol [Internet]. 2014 Feb 11 [cited 2014 Mar 22];3(1).

24. Baumal CR. Clinical applications of optical coherence tomography. Curr Opin Ophthalmol. 1999 Jun;10(3):182–188.

25. Drexler W, Fujimoto JG. State-of-the-art retinal optical coherence tomography. Prog Retin Eye Res. 2008 Jan;27(1):45–88.

26. Carmen K. M. C. The use of optical coherence tomography in neuro-ophthalmology. HKJOphthalmol. 15(1):12–19.

27. Dichtl A, Jonas JB, Naumann GOH. Histomorphometry of the optic disc in highly myopic eyes with absolute secondary angle closure glaucoma. Br J Ophthalmol. 1998 Mar 1;82(3):286–289.

28. Van Velthoven MEJ, Faber DJ, Verbraak FD, van Leeuwen TG, de Smet MD. Recent developments in optical coherence tomography for imaging the retina. Prog Retin Eye Res. 2007 Jan;26(1):57–77.

29. Samuel B, Rosario B, Bradley S. Tomografía De Coherencia Óptica. Atlas y Texto [Internet]. India by Nutech Print Services: Jaypee - Highlights Medical Publishers, INC.; 2009. 13-23 p.

30. Pagliara MM, Lepore D, Balestrazzi E. The role of OCT in glaucoma management. Prog Brain Res. 2008;173:139–148.

31. Keane PA, Sadda SR. Predicting visual outcomes for macular disease using optical coherence tomography. Saudi J Ophthalmol. 2011 Apr;25(2):145–158.

32. Liu Y-Y, Chen M, Ishikawa H, Wollstein G, Schuman JS, Rehg JM. Automated macular pathology diagnosis in retinal OCT images using multi-scale spatial pyramid and local binary patterns in texture and shape encoding. Med Image Anal. 2011 Oct;15(5):748–759.

33. Keane PA, Patel PJ, Liakopoulos S, Heussen FM, Sadda SR, Tufail A. Evaluation of Age-related Macular Degeneration With Optical Coherence Tomography. Surv Ophthalmol. 2012 Sep;57(5):389–414.

34. Alghadyan AA. Diabetic retinopathy – An update. Saudi J Ophthalmol. 2011 Apr;25(2):99–111.

35. Nicolò M, Zoli D, Musolino M, Traverso CE. Association Between the Efficacy of Half-Dose Photodynamic Therapy With Indocyanine Green Angiography and Optical Coherence Tomography Findings in the Treatment of Central Serous Chorioretinopathy. Am J Ophthalmol. 2012 Mar;153(3):474–480.e1.

36. Rahimy E, Beardsley RM, Gomez J, Hung C, Sarraf D. Grading of posterior staphyloma with spectral-domain optical coherence tomography and correlation with macular disease. Can J Ophthalmol J Can Ophtalmol. 2013 Dec;48(6):539–545.

37. Altemir I, Oros D, Elía N, Polo V, Larrosa JM, Pueyo V. Retinal asymmetry in children measured with optical coherence tomography. Am J Ophthalmol. 2013 Dec;156(6):1238–1243.e1.

38. Park JJ, Oh DR, Hong SP, Lee KW. Asymmetry analysis of the retinal nerve fiber layer thickness in normal eyes using optical coherence tomography. Korean J Ophthalmol KJO. 2005 Dec;19(4):281–287.

39. Sullivan-Mee M, Ruegg CC, Pensyl D, Halverson K, Qualls C. Diagnostic precision of retinal nerve fiber layer and macular thickness asymmetry parameters for identifying early primary open-angle glaucoma. Am J Ophthalmol. 2013 Sep;156(3):567–577.e1.

40. Turk A, Ceylan OM, Arici C, Keskin S, Erdurman C, Durukan AH, et al. Evaluation of the nerve fiber layer and macula in the eyes of healthy children using spectral-domain optical coherence tomography. Am J Ophthalmol. 2012 Mar;153(3):552–559.e1.

41. Mwanza J-C, Durbin MK, Budenz DL, Cirrus OCT Normative Database Study Group. Interocular symmetry in peripapillary retinal nerve fiber layer thickness measured with the Cirrus HD-OCT in healthy eyes. Am J Ophthalmol. 2011 Mar;151(3):514–521.e1.

42. Duan XR, Liang YB, Friedman DS, Sun LP, Wong TY, Tao QS, et al. Normal macular thickness measurements using optical coherence tomography in healthy eyes of adult Chinese persons: the Handan Eye Study. Ophthalmology. 2010 Aug;117(8):1585–1594.

43. Altemir I, Oros D, Elía N, Polo V, Larrosa JM, Pueyo V. Retinal asymmetry in children measured with optical coherence tomography. Am J Ophthalmol. 2013 Dec;156(6):1238–1243.e1.

44. Larsson E, Eriksson U, Alm A. Retinal nerve fibre layer thickness in full-term children assessed with Heidelberg retinal tomography and optical coherence tomography: normal values and interocular asymmetry. Acta Ophthalmol (Copenh). 2011 Mar;89(2):151–158.

45. Budenz DL. Symmetry between the right and left eyes of the normal retinal nerve fiber layer measured with optical coherence tomography (an AOS thesis). Trans Am Ophthalmol Soc. 2008;106:252–275.

46. Huynh SC, Wang XY, Burlutsky G, Mitchell P. Symmetry of optical coherence tomography retinal measurements in young children. Am J Ophthalmol. 2007 Mar;143(3):518–520.

9. ANNEXES

ANNEX I. INFORMED CONSENT

HOJA DE CONSENTIMIENTO INFORMADO

En cumplimiento de los artículos 8 y siguientes de la Ley 41/2002, de 14 de noviembre, básica reguladora de la autonomía del paciente y de derechos y obligaciones en materia de información y documentación clínica le ofrecemos por escrito y de manera comprensible la descripción de las características de riesgo y beneficios de participar en el proyecto de investigación cuyo objetivo es **determinar la asimetría de diversos parámetros fisiológicos de la retina mediante tomografía de coherencia óptica (3D OCT - 2000).**

Nombre del informador: **DOO. Zeyad Alzaben** Firma:_____

Descripción

Este proyecto de investigación está siendo realizado por Zeyad A. Alzaben, estudiante del máster de la Facultat d'Òptica i Optometria de Terrassa (Universidad Politécnica de Catalunya), dirigido por el Prof. Genís Cardona.

El propósito de esta investigación es **determinar la asimetría de diversos parámetros fisiológicos de la retina mediante tomografía de coherencia óptica (3D OCT - 2000).**

Usted es candidato para participar en este proyecto de investigación por tener retinas normales y ojos sanos.

Si acepta participar en este proyecto de investigación se le solicitará la realización de un conjunto de pruebas y la recolección de datos como su **refracción ocular , agudeza visual , parámetros de la retina** mediante la tomografía de coherencia óptica (prueba que permite adquirir, de forma no invasiva para el paciente sin aplicación de ningún colirio para la dilatación pupilar, y visualizar en tiempo real imágenes en alta resolución de la morfología retiniana, de la interfase vitreorretiniana y del segmento anterior). La participación en este estudio le tomará aproximadamente unos 30 min.

Riesgos y beneficios

No existen riesgos a nivel ocular durante la realización de este estudio dado que las pruebas que se realizan son empleadas en las consultas de optometría y oftalmología de manera cotidiana y todas ellas en este caso se realizan de manera NO invasiva.

Los beneficios esperados de esta investigación son su aportación a la ciencia, y la realización de distintas pruebas de tipo optométrico-oftalmológicas sin coste alguno.

Confidencialidad

La identidad del participante será protegida ya que todo este proceso será totalmente anónimo, solo se conocerá la edad y el sexo. Toda información o datos que pueda identificar al participante serán manejados confidencialmente.

Solamente el optometrista de este trabajo y los facultativos implicados en esta investigación tendrán acceso a los datos que puedan identificar directa o indirectamente a un participante, incluyendo esta hoja de consentimiento.

Estos datos serán almacenados en expedientes confidenciales con la finalidad única de esta investigación y se conservarán por un periodo de 2 años máximo después de que concluya este estudio.

Derechos

Si ha leído este documento y ha decidido participar, por favor entienda que su participación es completamente voluntaria y que usted tiene derecho a abstenerse de participar o retirarse del estudio en cualquier momento, sin ninguna penalidad. También tiene derecho a no participar en alguna prueba en particular. Además, tiene derecho a recibir una copia de este documento.

Si tiene alguna pregunta o desea más información sobre esta investigación, por favor comuníquese con XXXX al Tel. 97XXXX

Su firma en este documento significa que ha decidido participar después de haber leído y discutido la información presentada en esta hoja de consentimiento y que ha recibido copia de este documento.

Nombre de el/la participante	Firma	Fecha

Ha discutido el contenido de esta hoja de consentimiento con el/la arriba firmante

Nombre de el/la participante	Firma	Fecha